



**HAL**  
open science

# Seasonal variations of *Quercus pubescens* isoprene emissions from an in natura forest under drought stress and sensitivity to future climate change in the Mediterranean area

Anne-Cyrielle Genard-Zielinski, Christophe Boissard, Elena Ormeño, Juliette Lathiere, Ilja Reiter, Henri Wortham, Jean-Philippe Orts, Brice Temime-Roussel, Bertrand Guenet, Svenja Bartsch, et al.

## ► To cite this version:

Anne-Cyrielle Genard-Zielinski, Christophe Boissard, Elena Ormeño, Juliette Lathiere, Ilja Reiter, et al.. Seasonal variations of *Quercus pubescens* isoprene emissions from an in natura forest under drought stress and sensitivity to future climate change in the Mediterranean area. *Biogeosciences*, 2018, 15 (15), pp.4711-4730. 10.5194/bg-15-4711-2018 . hal-01876905

**HAL Id: hal-01876905**

**<https://amu.hal.science/hal-01876905v1>**

Submitted on 15 Mar 2019

**HAL** is a multi-disciplinary open access archive for the deposit and dissemination of scientific research documents, whether they are published or not. The documents may come from teaching and research institutions in France or abroad, or from public or private research centers.

L'archive ouverte pluridisciplinaire **HAL**, est destinée au dépôt et à la diffusion de documents scientifiques de niveau recherche, publiés ou non, émanant des établissements d'enseignement et de recherche français ou étrangers, des laboratoires publics ou privés.



## Seasonal variations of *Quercus pubescens* isoprene emissions from an *in natura* forest under drought stress and sensitivity to future climate change in the Mediterranean area

Anne-Cyrielle Genard-Zielinski<sup>1,2</sup>, Christophe Boissard<sup>2,3</sup>, Elena Ormeño<sup>1</sup>, Juliette Lathière<sup>2</sup>, Ilja M. Reiter<sup>4</sup>, Henri Wortham<sup>5</sup>, Jean-Philippe Orts<sup>1</sup>, Brice Temime-Roussel<sup>5</sup>, Bertrand Guenet<sup>2</sup>, Svenja Bartsch<sup>2</sup>, Thierry Gauquelin<sup>1</sup>, and Catherine Fernandez<sup>1</sup>

<sup>1</sup>Aix Marseille Université, Avignon Université, CNRS, IRD, IMBE, Institut Méditerranéen de Biodiversité et d'Ecologie marine et continentale, Marseille, 13331, France

<sup>2</sup>Laboratoire des Sciences du Climat et de l'Environnement, LSCE/IPSL, CEA-CNRS-UVSQ, Université Paris-Saclay, Gif-sur-Yvette, 91191, France

<sup>3</sup>Université Paris Diderot, Paris 7, Paris, 75013, France

<sup>4</sup>Fédération de Recherche "Ecosystèmes Continentaux et Risques Environnementaux", CNRS FR 3098 ECCOREV, Technopôle de l'environnement Arbois-Méditerranée, Aix-en-Provence, 13545, France

<sup>5</sup>Aix Marseille Université, CNRS, LCE, Laboratoire de Chimie de l'Environnement, Marseille, 13331, France

**Correspondence:** Christophe Boissard (christophe.boissard@lsce.ipsl.fr)

Received: 24 January 2017 – Discussion started: 9 February 2017

Revised: 5 July 2018 – Accepted: 7 July 2018 – Published: 3 August 2018

**Abstract.** At a local level, biogenic isoprene emissions can greatly affect the air quality of urban areas surrounded by large vegetation sources, such as in the Mediterranean region. The impacts of future warmer and drier conditions on isoprene emissions from Mediterranean emitters are still under debate. Seasonal variations of *Quercus pubescens* gas exchange and isoprene emission rates (ER) were studied from June 2012 to June 2013 at the O<sub>3</sub>HP site (French Mediterranean) under natural (ND) and amplified (AD, 32 %) drought. While AD significantly reduced stomatal conductance to water vapour throughout the research period excluding August, it did not significantly preclude CO<sub>2</sub> net assimilation, which was lowest in summer ( $\approx -1 \mu\text{molCO}_2 \text{ m}^{-2} \text{ s}^{-1}$ ). ER followed a significant seasonal pattern regardless of drought intensity, with mean ER maxima of 78.5 and 104.8  $\mu\text{gC g}_{\text{DM}}^{-1} \text{ h}^{-1}$  in July (ND) and August (AD) respectively and minima of 6 and  $< 2 \mu\text{gC g}_{\text{DM}}^{-1} \text{ h}^{-1}$  in October and April respectively. The isoprene emission factor increased significantly by a factor of 2 in August and September under AD (137.8 and 74.3  $\mu\text{gC g}_{\text{DM}}^{-1} \text{ h}^{-1}$ ) compared with ND (75.3 and 40.21  $\mu\text{gC g}_{\text{DM}}^{-1} \text{ h}^{-1}$ ), but no significant changes occurred on ER. Aside from the June 2012

and 2013 measurements, the MEGAN2.1 (Model of Emissions of Gases and Aerosols from Nature version 2.1) model was able to assess the observed ER variability only when its soil moisture activity factor  $\gamma_{\text{SM}}$  was not operating and regardless of the drought intensity; in this case more than 80 % and 50 % of ER seasonal variability was assessed in the ND and AD respectively. We suggest that a specific formulation of  $\gamma_{\text{SM}}$  be developed for the drought-adapted isoprene emitter, according to that obtained for *Q. pubescens* in this study ( $\gamma_{\text{SM}} = 0.192e^{51.93 \text{ SW}}$  with SW the soil water content). An isoprene algorithm (*G14*) was developed using an optimised artificial neural network (ANN) trained on our experimental dataset (ER + O<sub>3</sub>HP climatic and edaphic parameters cumulated over 0 to 21 days prior to the measurements). *G14* assessed more than 80 % of the observed ER seasonal variations, regardless of the drought intensity. ER<sub>*G14*</sub> was more sensitive to higher (0 to  $-7$  days) frequency environmental changes under AD in comparison to ND. Using IPCC RCP2.6 and RCP8.5 climate scenarios, and SW and temperature as calculated by the ORCHIDEE land surface model, ER<sub>*G14*</sub> was found to be mostly sensitive to future temperature and nearly insensitive to precipitation decrease (an annual increase of up to 240 % and at the most 10 % respectively in the

most severe scenario). The main impact of future drier conditions in the Mediterranean was found to be an enhancement (+40 %) of isoprene emissions sensitivity to thermal stress.

## 1 Introduction

A large number of Mediterranean deciduous and evergreen trees produce and release isoprene (2-methyl-1,3-butadiene, C<sub>5</sub>H<sub>8</sub>). Under non-stress conditions, only 1 %–2 % of the carbon recently assimilated is emitted as isoprene, whereas under stress conditions such as water scarcity this value can reach up to 20 %–30 % (*Quercus pubescens*, Genard-Zielinski et al., 2014). Although the role of isoprene remains a subject of debate, it seems likely that C<sub>5</sub>H<sub>8</sub> helps plants to optimise CO<sub>2</sub> assimilation during temporary and mild stresses, especially during the growing and warmer periods (Brilli et al., 2007; Loreto and Fineschi, 2015). The major role of isoprene in plant defence probably explains its large annual global emissions (440–660 TgC yr<sup>-1</sup>, Guenther et al., 2006), forming the largest quantity of all biogenic volatile organic compounds (BVOCs) emitted. Although present in the atmosphere at the ppb or ppt level, isoprene has a broad impact on atmospheric chemistry, both in the gas phase (especially in the O<sub>3</sub> budget of some urbanised areas, Atkinson and Arey, 2003) and in the particulate phase (secondary organic aerosols formation, Goldstein and Steiner, 2007), and hence on biosphere–atmosphere feedbacks. For instance, in the Mediterranean area, Curci et al. (2009) showed that isoprene could be responsible for the production of 4 to 6 ppbv of ozone between June and August, representing 16 %–20 % of total ozone. Given the broad impacts of isoprene on atmospheric chemistry, considerable efforts have been made to (i) understand the physiological mechanisms responsible for isoprene synthesis and emission and the different environmental parameters that control their variability, in order to (ii) develop isoprene emission models that can account for the broadest possible range of environmental conditions.

Thus, it has extensively been shown that under non-stressful conditions, isoprene synthesis and emission are closely connected and primarily depend upon light and temperature conditions (Guenther et al., 1991, 1993). In contrast, under environmental stress, isoprene emission and synthesis are uncoupled in a way that is not fully understood and hence still under debate (Affek and Yakir, 2003; Peñuelas and Staudt, 2010). Indeed, although some authors have identified an increase in isoprene emission under mild water stress (Sharkey and Loreto, 1993; Funk et al., 2004; Pegoraro et al., 2004; Genard-Zielinski et al., 2014), others have reported the opposite (Brüggemann and Schnitzler, 2002; Rodriguez-Calcerrada et al., 2013; Tani et al., 2011).

Concerning the modelling of isoprene emission variations, two main approaches have been considered so far: (i) empirically based parameterisations to represent observed emis-

sion variations in relation to easily accessible environmental drivers and (ii) process-based relationships built on the understanding of the ongoing biological regulation (see Ashworth et al., 2013). Both types of model are adapted for global and regional modelling, but the former are more commonly used for atmospheric applications, especially for air quality exercises for which mechanistic models remain far too complex. Indeed, whilst Grote et al. (2014) have indicated that such models are fairly effective in accounting for the mild stress effects on seasonal isoprene variations of *Quercus ilex*, the large number of necessary descriptive parameters continues to represent an obstacle for their broad and routine use in air quality (Ashworth et al., 2013). Moreover, the development of BVOC empirical emission models, and especially of the most widely used empirical model, MEGAN (Model of Emissions of Gases and Aerosols from Nature, Guenther et al., 2006, 2012), was partly based on measurements carried out under optimum growing conditions and/or obtained from very few emitters. Therefore, if they depict a fair picture of the general level and global distribution of BVOC emission, they remain somewhat deficient in accounting for a large range of stress conditions. When used for air quality monitoring applications, such a bias intrinsic to the model can significantly weaken air quality forecasts in areas that are greatly influenced by biogenic sources (von Kuhlmann et al., 2004; Chaxel and Chollet, 2009). Concerning the impact of drought stress, the inclusion of the soil moisture effect on isoprene emission in MEGAN was derived from a sole drought study made on *Populus deltoides* (Pegoraro et al., 2004). Validation regarding a broader range of environmental conditions (including stress conditions) and emitters is necessary. Weaknesses in accounting for the impact of drought can be detrimental to isoprene emission inventories, especially when undertaken in areas that are covered with a large quantity of high isoprene emitters and that are subject to frequent drought episodes, like the Mediterranean region. Moreover, in addition to a predicted temperature increase of between 1.5 and 3 °C, climate models over this area predict an amplification of the natural drought (ND) during summers due to a reduction in precipitation that could locally reach up to 30 % by the year 2100 (Giorgi and Lionello, 2008; Intergovernmental Panel on Climate Change, 2013; Polade et al., 2014). Owing to the close interactions between air pollution over large Mediterranean urban areas and strong BVOC emissions from nearby vegetation, the potential impacts of future climatic changes on isoprene emissions represent an acute environmental issue needing to be addressed (Chameides et al., 1988; Atkinson and Arey, 1998; Calfapietra et al., 2009; Pacifico et al., 2009). Within this context, a recent study has underlined the importance of monitoring over a long period both isoprene emissions and soil moisture in water-limited ecosystems (Zheng et al., 2015). Since *Q. pubescens* Willd. is the second largest isoprene emitter in Europe (and foremost in the Mediterranean zone) (Keenan et al., 2009), it represents an ideal model

species by which to investigate isoprene emission variability under drought conditions.

The objectives of this study were (i) to investigate *in natura* the influence of natural (ND) and amplified (AD) drought on *Q. Pubescens* seasonal gas exchanges ( $\text{CO}_2$ ,  $\text{H}_2\text{O}$ ) and in particular isoprene emission rates (ER); (ii) to test and compare two empirical emission models, MEGAN2.1 (Guenther et al., 2012) and *G14* (this study) in assessing seasonal ER variability under different drought intensities; and (iii) to evaluate the sensitivity of ER to future climatic changes (warming and precipitation reduction) based on two extreme IPCC scenarios: RCP2.6 (moderate) and RCP8.5 (extreme).

## 2 Materials and methods

### 2.1 Experimental site O<sub>3</sub>HP

Experimental data were obtained at the O<sub>3</sub>HP site (Oak Observatory at the Observatoire de Haute Provence, 5°42'44" E, 43°55'54" N). This site constitutes part of the French national network SOERE F-ORE-T (System of Observation and Experimentation, in the long term, for Environmental Research) dedicated to investigating the functioning of the forest ecosystem. The O<sub>3</sub>HP site (680 m above mean sea level) is located 60 km north of Marseille and consists of a homogeneous 70–100-year-old coppice dominated by *Q. pubescens* (5 m in height; leaf area index, LAI = 2.2), which accounts for  $\approx 90\%$  of the biomass and  $\approx 75\%$  of the trees. A rainout shelter above 300 m<sup>2</sup> of the canopy dynamically excluded rainfall by deploying automated shutters. This facility facilitated the study of *Q. pubescens* under natural and amplified drought, henceforth referred to as the ND and AD plot respectively. In the present study, the device was deployed during rain events from the end of May until October 2012 in order to exclude 32% of the precipitation in the rain exclusion plot. In practice, almost all rainfall in late spring and summer was thus intercepted, increasing the number of dry days (< 1 mm, Polade et al., 2014) by 22. This percentage corresponds with the highest IPCC projections made for the end of the century over the Mediterranean area and accords with the precipitation reduction at O<sub>3</sub>HP during the driest years from 1967 to 2000 compared with the average precipitation over this period. Using an ombrothermic diagram ( $P < 2T$ , with  $P$  = monthly precipitation in mm and  $T$  = monthly air temperature in °C), we assessed that the summer 2012 drought period reaches 4.5 months in the AD plot, compared with 3 months in the ND plot. Ambient and soil environmental parameters were continuously monitored using a dense network of sensors (for details see Sect. 2.7). Access to the canopy was at two levels:  $\approx 0.8$  and 3.5 m (top canopy branches) above ground level, with the highest level being the one at which we undertook this study. Further description can be found in Santonja et al. (2015).

### 2.2 Seasonal sampling strategy

Isoprene emission rate measurements were undertaken for at least 1 week per month from June 2012 to June 2013, except for the period from November 2012 until March 2013 when *Q. pubescens* is fully senescent, with leaves remaining on the tree (marcescent species). This calendar enabled us to capture isoprene emissions during leaf maturity but also during bud break (April 2013) and just before leaf senescence (October 2012). Three trees were studied in each plot along the whole seasonal cycle, with a single branch at the top of the canopy predominantly sampled for each tree. More intensive measurements were carried out in June 2012 (3 weeks) and April 2013 when tree-to-tree and within-canopy variability was assessed. One ND branch was subsequently sampled throughout all intensive campaigns, and the five other ND and AD branches were alternately sampled during 1 to 2 days (Genard-Zielinski et al., 2015). Isoprene samples were collected on cartridges packed with adsorbents, apart from April 2013 when online isoprene measurements were conducted using a PTR-MS (proton-transfer-reaction mass spectrometer) directly connected to the enclosure via a 50 m 1/4" PTFE line. When cartridges were used, samples (volume ranging between 0.45 and 0.9 L, depending on the expected emission intensity) were taken from sunrise to sunset, roughly every 2 h. PTR-MS measurements allowed a higher sampling frequency (between 120 and 390 s<sup>-1</sup>).

Branch enclosures were generally installed on the day before the first emission rate measurement was taken and at least 2 h beforehand in order for the plant to return to normal physiological functioning. Note that although senescence had just begun in October 2012, we did check that the enclosed branches were not senescent during these measurements.

### 2.3 Branch-scale isoprene emissions and gas exchanges

Sampling was undertaken using two identical dynamic branch enclosures (detailed description in Genard-Zielinski et al., 2015). Briefly, the device consisted of a  $\approx 60$  L PTFE (polytetrafluoroethylene) frame closed by a sealed, 50  $\mu\text{m}$  thick PTFE film, to which ambient air was introduced at  $Q_0$  ranging between 11 and 14 L min<sup>-1</sup> using a PTFE pump (KNF N 840.1.2 FT.18<sup>®</sup>, Germany). Gas flow rates were controlled by mass flow controllers (Bronkhorst) and all tubing lines were made of PTFE. A PTFE propeller ensured the rapid mixing of air inside the chamber. The microclimate (PAR, photosynthetic active radiation;  $T$ ; relative humidity) inside the chamber was continuously monitored (relative humidity and temperature probe LI-COR 1400–104<sup>®</sup>, and quantum sensor LI-COR, PAR-SA 190<sup>®</sup>; Lincoln, NE, USA) and recorded (LI-COR 1400<sup>®</sup>; Lincoln, NE, USA).  $\text{CO}_2$ – $\text{H}_2\text{O}$  exchanges from the enclosed branches were also continuously measured using infrared gas analysers (IRGA 840A<sup>®</sup>, LI-COR) in order to assess the net assimilation  $P_n$

(in  $\mu\text{molCO}_2 \text{ m}^{-2} \text{ s}^{-1}$ ) and the stomatal conductance to water vapour  $G_w$  ( $\text{molH}_2\text{O} \text{ m}^{-2} \text{ s}^{-1}$ ) using the equations from Von Caemmerer and Farquhar (1981) as detailed in Genard-Zielinski et al. (2015).

Total dry biomass matter (DM) was calculated by manually scanning every leaf of each sampled branch enclosed in the chamber and applying a dry leaf mass per area conversion factor (LMA) extrapolated from concomitant measurements made on the same site. The mean (range) DM was 0.16 (0.01–0.45)  $\text{g}_{\text{DM}}$ , and mean (range) LMA was 13.17 (0.82–36.67)  $\text{g}_{\text{DM}} \text{ cm}^{-2}$ .

Isoprene emission rates (ER) were calculated as

$$\text{ER} = Q_0 \times (C_{\text{out}} - C_{\text{in}}) \times \text{DM}^{-1}, \quad (1)$$

where ER is expressed in  $\mu\text{gC g}_{\text{DM}}^{-1} \text{ h}^{-1}$ ,  $Q_0$  is the flow rate of the air introduced into the chamber ( $\text{L h}^{-1}$ ),  $C_{\text{in}}$  and  $C_{\text{out}}$  are the concentrations in the inflowing and outflowing air ( $\mu\text{gC L}^{-1}$ ), and DM is the sampled dry biomass matter ( $\text{g}_{\text{DM}}$ ).

Throughout the seasonal cycle, except in April, isoprene was collected using packed cartridges (glass and stainless-steel) prefilled with Tenax TA and/or Carbotrap. Isoprene was then analysed in the laboratory according to a gas chromatography–mass spectrometry (GM-MS) procedure detailed in Genard-Zielinski et al. (2015), with a level of analytical precision greater than 7.5 %.

In April 2013, two types of PTR-MS were used for on-line isoprene sampling and analysis. A quadrupole PTR-MS (HS-PTR-MS, Ionicon Analytik GmbH, Innsbruck Austria), connected to the ND branch enclosure, was operated at 2.2 mbar pressure, 60 °C temperature, and 500 V voltage in order to achieve an  $E/N$  ratio of  $\approx 115 \text{ Td}$  ( $E$ : electric field strength ( $\text{V cm}^{-1}$ );  $N$ : buffer gas number density ( $\text{molecule cm}^{-3}$ );  $1 \text{ Td} = 10^{-17} \text{ V cm}^2$ ). The primary  $\text{H}_3\text{O}^+$  ion count assessed at  $m/z$  21 was  $3 \times 10^7$  cps, with a typically < 10 % contribution monitored from the first water cluster ( $m/z$  37) and < 5 % contribution from the  $\text{O}_2^+$  ( $m/z$  32). Measurements were operated in scan mode ( $m/z$  21 to  $m/z$  210) every 380 s. After 15–20 min of sampling of incoming air, the outgoing air was sampled for 30 to 60 min. A high-resolution ( $m/\Delta m \approx 4000$ ) time-of-flight PTR-MS (PTR-ToF-MS-8000, Ionicon Analytik GmbH, Innsbruck Austria) connected to the second enclosure used in our study enabled us to discriminate between compounds when their masses differ at the tenth part. The main experimental characteristics were similar to the HS-PTR-MS, but a voltage of 550 V was used in order to reach an  $E/N$  ratio of  $\approx 125 \text{ Td}$ . The  $\text{H}_3\text{O}^+$  ion count assessed at  $m/z$  21 was  $1.1 \times 10^6$  cps with a similar < 10 % contribution monitored from the first water cluster ( $m/z$  37) and < 2.5 % contribution from the  $\text{O}_2^+$  ( $m/z$  32). The signal at  $m/z$  69 corresponding to protonated isoprene was converted into mixing ratio by using a proton transfer rate constant  $k$  of  $1.96 \times 10^{-9} \text{ cm}^3 \text{ s}^{-1}$  (Cappellin et al., 2012), the reaction time in the drift tube, and the experimentally determined ion transmission efficiency. The relative ion

transmission efficiencies of both instruments were assessed using a standard gas calibration mixture (TO-14A Aromatic Mix, Restek Corporation, Bellefonte, USA;  $100 \pm 10$  ppb in nitrogen). Assuming an uncertainty of  $\pm 15$  % in the  $k$ -rate constants and in the mass transmission efficiency, the overall uncertainty of the concentration measurement is estimated to be of the order of  $\pm 20$  %. Background signal was obtained by passing air through a platinum catalytic converter heated at 300 °C. Detection limits defined as 3 times the standard deviation on the background signal were 10 and 50 ppt with the PTR-ToF-MS and the HS-PTR-MS respectively. An intercomparison between both the cartridge + GC-MS and PTR-MS protocols was undertaken parallel to another emitter present on the site (*Acer monspessulanum*); no significant difference was observed between the techniques (Genard-Zielinski et al., 2015).

The overall uncertainty (sampling + analysis) on ER assessment was between 20 % and 25 %.

## 2.4 Statistics

All statistics were performed on STATGRAPHICS® centurion XV by Statpoint, Inc. Differences in  $P_n$ ,  $G_w$ , ER, and *Q. pubescens* isoprene emission factors ( $\varepsilon_{\text{iso}, \text{Qp}}$ , see Sect. 2.5 for details) between the ND and the AD plot were tested using Mann–Whitney  $U$  tests. Seasonal changes in these ecophysiological parameters were tested using the Kruskal–Wallis test and the analysis was performed separately on trees from the ND and AD plot. Comparisons between COOPERATE environmental data (see Sect. 2.7) were made using a Wilcoxon test when data were not log-normal and a  $t$  test when log-normal.

## 2.5 Branch-scale ER assessment using MEGAN2.1 emission model

Based on the latest version of the MEGAN model (MEGAN2.1, Guenther et al., 2012), *Q. pubescens* ER were assessed for the sampling conditions of our seasonal study using

$$\text{ER}_{\text{MEGAN}} = \varepsilon_{\text{iso}, \text{Qp}} \chi_{\text{Qp}} \gamma_{\text{iso}}. \quad (2)$$

Nota bene: in order to be comparable with our measurements carried out on top canopy leaves and expressed as net emission rates in the unit of  $\mu\text{gC g}_{\text{DM}}^{-1} \text{ h}^{-1}$ , no canopy environment coefficient  $C_{\text{CE}}$  nor LAI was considered in the calculation of  $\gamma_{\text{iso}}$  and thus in  $\text{ER}_{\text{MEGAN}}$  (for further details see Guenther et al., 2012).

## 2.6 Branch-scale ER assessment using an artificial neural network trained on field data

The artificial neural network (ANN) developed in this study to assess branch-scale ER from *Q. pubescens* (henceforth referred to as *G14*) was based on a commercial version of

the Netral NeuroOne software v.6.0 (<http://www.inmodelia.com/>, France; last access: 31 July 2018). The ANN was used as a multilayer perceptron (MLP) in order to calculate multiple non-linear regressions between a set of input regressors  $x_i$  (the environmental variables measured at the O<sub>3</sub>HP) and the output data (the measured isoprene ER). The assessed ER (ER<sub>G14</sub>) was calculated as follows:

$$\text{ER}_{G14} = w_0 + \sum_{j=1}^{j=N} \left[ w_{j,k} \times f \left( w_{0,j} + \sum_{i=1}^{i=n} w_{i,j} \times x_i \right) \right], \quad (3)$$

where  $w_0$  is the connecting weight between the bias and the output,  $N$  the number of neurons  $N_j$ ,  $f$  the transfer function,  $w_{0,j}$  the connecting weight between the bias and the neuron  $N_j$ ,  $w_i$  the connecting weight between the input and the neuron  $N_j$ , and  $x_i$  the  $n$  input regressors. The MLP optimisation of the weights  $w$  was achieved according to Boisard et al. (2008). Every input regressor  $x_i$  was centrally normalised. Two sub-datasets were considered, for the ND and AD plot respectively. For each sub-dataset, 80 % of our data were used for training and optimising the MLP, and the remaining 20 % were used for blind validation based on root mean square error (RMSE). Training–validation splitting was made using a Kullback–Leibler distance function available in NeuroOne v 6.0. Only the non-linear hyperbolic tangent (tanh) function was tested as transfer function  $f$ . Up to  $N = 7$  neurons (distributed in only one layer) were tested for every ANN setting. The overtraining phenomenon (a too-large number of neurons vs. the number of input parameters) was checked against the  $\text{RMSE}_{\text{training}}/\text{RMSE}_{\text{validation}}$  evolution vs. the number  $N$  of neurons tested: training was stopped for  $\text{RMSE}_{\text{training}} > \text{RMSE}_{\text{validation}}$  when  $N \geq 3$ .

Among the other available statistical methods, ANNs present the advantage of being the most parsimonious, i.e., giving the smallest error for a same number of descriptors (see for instance Dreyfus et al., 2002). Moreover, the ANN approach, as is the case of other non-linear regression methods, is not particularly sensitive to regressors' co-linearity (Bishop, 1995; Dreyfus et al., 2002). On the other hand, one of the limitations of ANNs is that they can only be employed for interpolation within the range of values of the trained data, and not for extrapolation exercises beyond this range. Consequently, during the isoprene emission sensitivity to future climatic changes (see Sect. 2.8), only  $x_i$  values fitting within the range of variation ( $\pm 20\%$ ) tested during the training phase were considered; in total 21 % of the data were thus rejected.

## 2.7 COOPERATE environmental database

Ambient and edaphic parameters used for the ANN optimisation were obtained from the COOPERATE database (<https://cooperate.obs-hp.fr/db>, last access: 31 July 2018) and daily averaged for each day of our study. Ambient PAR ( $\mu\text{mol m}^{-2} \text{s}^{-1}$ ) measured above the canopy at 6.5 m (LICOR Li-190®; Lincoln, NE, USA) in the ND plot was used

as the PAR reaching all of the top canopy branches studied. Ambient air temperature ( $T$ , °C) measured at 6.15 m (CS215, Campbell Scientific Ltd., UK) in the ND and AD plot was used for both sets of branches. Since some precipitation ( $P$ , mm) values were missing (< 5 %) from the COOPERATE database during our data processing,  $P$  values from the nearby (< 10 km) Forcalquier meteorological station were used. The bias between cumulated  $P$  ( $P_{\text{cum}}$ ) curves at both sites was assessed and considered in order to extrapolate the missing values at the O<sub>3</sub>HP site. As  $P$  was cumulated over 7, 14, and 21 days, the resulting bias was negligible ( $\approx 1\%$ ) and no further adjustment was made. Soil water content (SW,  $\text{L L}^{-1}$ ) and temperature (ST, °C) at  $-0.1$  m (Hydra Probe II, Stevens, Water Monitoring Systems Inc., OR, USA) specific to each of the sampled trees were selected and extracted from the COOPERATE database; when soil data were missing, they were extrapolated from the nearest equivalent data point measurement. Daily mean PAR,  $T$ ,  $P$ , SW, and ST were cumulated over a time period ranging from 1 to 21 days before the measurement.

## 2.8 ORCHIDEE land surface model: providing future conditions to investigate ER sensitivity to climatic changes

Present-day  $T$  and  $P$  were assessed as the 2000–2010 daily averages derived from the ISI-MIP (Inter-Sectoral Impact Model Intercomparison Project) climate dataset (Warszawski et al., 2014) over the Mediterranean area. This dataset contains the bias-corrected daily simulation outputs of the Earth system model HadGEM2-ES. Corresponding values for the 2090–2100 period were used to assess the expected range of future climatic changes. They were derived from two ISI-MIP future projections forced along two representative concentration pathways (RCPs): the so-called “peak-and-decline” greenhouse gas concentration scenario RCP2.6 (optimistic or moderate scenario) and the “rising” greenhouse gas concentration scenario RCP8.5 (extreme or severe scenario). All  $T$  and  $P$  data were extracted for the entire Mediterranean region from the global ISI-MIP dataset and subsequently averaged over the area.

Using these present and future  $T$ ,  $P$ , and PAR values (ISI-MIP derived), the corresponding present and future SW and ST were assessed by running the global land surface model ORCHIDEE (ORGanising Carbon and Hydrology In Dynamic EcosystEms) over the European part of the Mediterranean region. The calculated SW and ST were averaged over this area. ORCHIDEE is a spatially explicit, process-based model that calculates the CO<sub>2</sub>, H<sub>2</sub>O, and heat fluxes between the land surface and the atmosphere. Vegetation species distributed at the Earth's surface are represented in ORCHIDEE through 13 plant functional types (PFTs). Processes in the model are represented at the time step of 0.5 h, but the variations of water and carbon pools are calculated on a daily basis. A detailed description of ORCHIDEE is

provided by Krinner et al. (2005). Simulations over the European part of the Mediterranean region were performed with the ORCHIDEE model at  $0.5 \times 0.5^\circ$  spatial resolution using the soil parameters (clay, silt, and sand fractions) from Zabler (1986). Given that this study focuses on isoprene emissions from *Q. pubescens*, we fixed the vegetation with the corresponding PFT “temperate broad-leaf summer green tree”. The described ISI-MIP historical forcings and the ISI-MIP future projections were used as climate conditions for ORCHIDEE runs and ER assessment using G14. Equilibrium was reached by running ORCHIDEE on the first decade of the climate forcing (1961–1990) repeated in a loop and the value of atmospheric  $\text{CO}_2$  corresponding to the year 1961. Among the two different hydrology schemes available in ORCHIDEE, the physically based 11-layer scheme was used (Guimberteau et al., 2013).

ER sensitivity to moderate and severe temperature and/or precipitation changes was evaluated using G14 under 6 cases: (i) the  $T$  (respectively  $P$ ) test was conducted considering only  $T$  and ST (respectively only  $P$  and SW) changes according to the RCP2.6 scenario; (ii) the  $TT$  and  $PP$  tests were similar to the  $T$  and  $P$  tests but considered changes according to the RCP8.5 scenario; (iii) the  $T + P$  (respectively  $TT + PP$ ) test combined the effect of  $T$ , ST,  $P$ , and SW changes according to RCP2.6 (respectively RCP8.5).

### 3 Results

#### 3.1 Environmental conditions observed at the O<sub>3</sub>HP

Mean daily ambient air temperature  $T$  varied between  $-3$  and  $26^\circ\text{C}$  (January 2013 and August 2012 respectively, Fig. 1a). Seasonal PAR variations were in line with  $T$  variations, with the daily mean peaking at  $900 \mu\text{mol m}^{-2} \text{s}^{-1}$  in July (Fig. 1b). In 2012, the amplification of the ND was adjusted from May to reach its maximum (32%) in July and maintained until November when rain exclusion was stopped (Fig. 1c). The annual  $P_{\text{cum}}$  in the AD plot was lower by 273 mm than in the ND plot at the end of 2012 (782 compared to 509 mm). In 2013 the AD started only at the end of June, simulating a later amplification. From August until October 2012, SW was 50%–90% lower in the AD plot than in the ND plot ( $\approx 0.02$  and to  $0.05 \text{ L}_{\text{H}_2\text{O}} \text{ L}_{\text{soil}}^{-1}$  respectively in August, Fig. 1d). The AD plot soil water deficit remained significant until the end of the experiment (Mann–Whitney,  $P < 0.05$  in June 2012,  $P < 0.001$  from July 2012 to June 2013), although the rain exclusion system was not activated between December 2012 and June 2013.

No significant difference was noticed for monthly PAR and  $T$  means between the ND and the AD plot, except in September 2012 when branches sampled on the ND plot received significantly more PAR than branches on the AD plot (Mann–Whitney,  $P < 0.001$ ). This difference could be due to an orientation of the branches sampled in the ND plot in

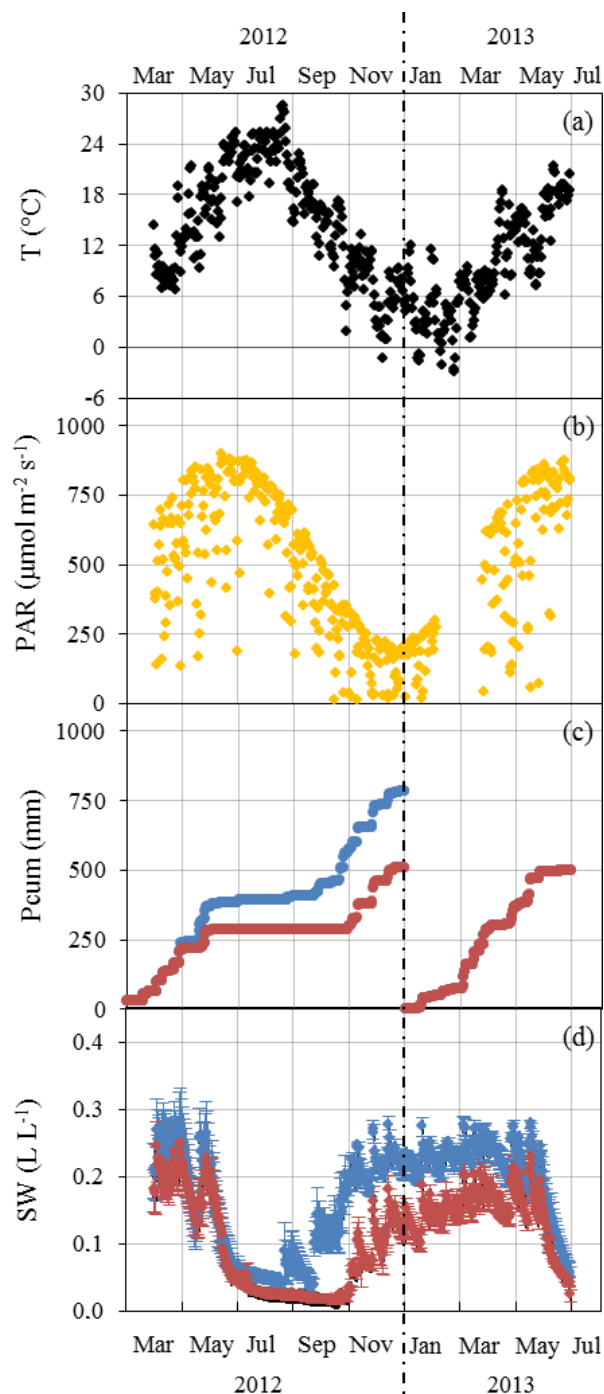


**Figure 1.** Seasonal variations of daily environmental parameters measured at the O<sub>3</sub>HP from March 2012 to June 2013. (a) Ambient air temperature  $T$  was obtained at 6.5 m above ground level (a.g.l.), approximately 1.5 m above the canopy. (b) Photosynthetic active radiations PAR received at 6.5 m a.g.l. in the ND plot. (c) Cumulated precipitation  $P_{\text{cum}}$  measured over the ND (blue) and AD (red) plot. (d) Mean soil water content  $\text{SW} \pm \text{SD}$  measured at  $-0.1$  m depth from various soil probes in the ND (blue,  $n = 3$ ) and AD (red,  $n = 5$ ) plot.

September that enabled greater receipt of PAR during our measurements than the AN sampled branches.

### 3.2 Gas exchange and isoprene seasonal variations

$G_w$  and  $P_n$  showed similar seasonal patterns in both plots (Fig. 2a, b), with the lowest values in July–September ( $10\text{--}20\text{ mol}_{\text{H}_2\text{O}}\text{ m}^{-2}\text{ s}^{-1}$  and  $\approx 1\text{ }\mu\text{mol}_{\text{CO}_2}\text{ m}^{-2}\text{ s}^{-1}$  respectively) and the highest in June ( $80\text{--}170\text{ mol}_{\text{H}_2\text{O}}\text{ m}^{-2}\text{ s}^{-1}$  and  $\approx 9\text{ }\mu\text{mol}_{\text{CO}_2}\text{ m}^{-2}\text{ s}^{-1}$  respectively). Respiration dominated over gross  $\text{CO}_2$  assimilation in April, resulting in negative net assimilation ( $P_n \approx -1\text{ }\mu\text{mol}_{\text{CO}_2}\text{ m}^{-2}\text{ s}^{-1}$ ) in both plots. In contrast,  $G_w$  and  $P_n$  were not influenced by water stress in the same way. Whereas  $G_w$  was significantly reduced under AD from July 2012,  $P_n$  remained stable, except in June 2013 when  $P_n$  values that were twice as high under AD than ND were observed. It is important to note that the tomography measurements made at this site showed that oak roots were predominantly distributed in the outermost humiferous horizon located above a calcareous slab at a 10–20 cm depth and that only very few roots crossed this slab.

Water stress only affected the ER seasonal pattern during summer (Fig. 2c). Maximum ER was delayed by a month in the AD plot ( $104.8\text{ }\mu\text{gC g}_{\text{DM}}^{-1}\text{ h}^{-1}$  in August) in comparison to the ND plot ( $78.5\text{ }\mu\text{gC g}_{\text{DM}}^{-1}\text{ h}^{-1}$  in July). ER was lowest in October ( $\approx 6\text{ }\mu\text{gC g}_{\text{DM}}^{-1}\text{ h}^{-1}$  in both plots). During April bud break and isoprene emission onset, ER was as low as 0.5 and  $1\text{ }\mu\text{gC g}_{\text{DM}}^{-1}\text{ h}^{-1}$  in the ND and AD plot respectively.

Although  $\varepsilon_{\text{iso,QP}}$  was calculated every month as the slope of ER vs.  $C_L \times C_T$  (as in Guenther et al., 1995), this correlation was not significant in July, especially in the case of AD branches ( $P > 0.05$ ,  $R^2 = 0.06$  and  $0.01$  for ND and AD respectively). As a result,  $\varepsilon_{\text{iso,QP}}$  in July was calculated by averaging ER measured under environmental conditions close to  $1000 \pm 100\text{ }\mu\text{mol m}^{-2}\text{ s}^{-1}$  and  $30 \pm 1\text{ }^\circ\text{C}$ . In general, AD branches showed poorer ER vs.  $C_L \times C_T$  correlations than branches growing in the ND plot (data not shown).  $\varepsilon_{\text{iso,QP}}$  was significantly higher by a factor of 2 in August and September for the AD branches compared to the ND (Fig. 2d). As for ER,  $\varepsilon_{\text{iso,QP}}$  maximum was reached in August ( $137.8\text{ }\mu\text{gC g}_{\text{DM}}^{-1}\text{ h}^{-1}$ ) in the AD plot, while the maximum in the ND plot occurred in July ( $74.3\text{ }\mu\text{gC g}_{\text{DM}}^{-1}\text{ h}^{-1}$ ). The general high variability observed in April during the isoprene emission onset (some branches were already emitting, while some were not yet emitting isoprene, regardless of their locations in the AD/ND plots) was as large as the AD–ND variability and thus could not solely be attributed to the water stress treatment. The relative annual  $\varepsilon_{\text{iso,QP}}$  difference between ND and AD was +45 %.

### 3.3 Modelling the isoprene seasonal variations of *Q. pubescens* at the O<sub>3</sub>HP

Given that we were aiming to test the capacity of an empirically based isoprene emission model to describe seasonal

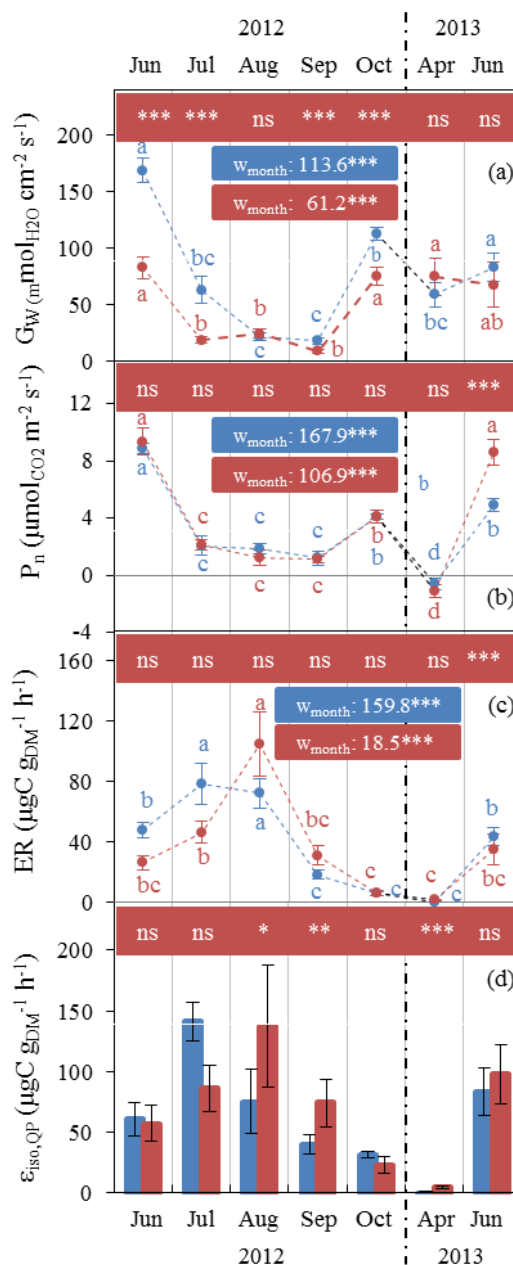


**Figure 2.** Seasonal variations of monthly *Q. pubescens* gas exchanges observed at O<sub>3</sub>HP (June 2012 to June 2013) under ND (blue) and AD (red) (mean  $\pm$  SD). (a) Stomatal conductance to water vapour  $G_w$ . (b) Net photosynthetic assimilation  $P_n$ . (c) Measured branch isoprene emission rate ER. (d) Isoprene emission factor ( $I_s$ ) calculated according to Guenther et al. (1995) using in situ ER vs.  $C_L \times C_T$  correlations, except in July where mean ER measured under enclosure conditions close to  $1000\text{ }\mu\text{mol m}^{-2}\text{ s}^{-1}$  and  $30\text{ }^\circ\text{C}$  was used. Differences between ND and AD using Mann–Whitney  $U$  tests are denoted using lower case letters ( $a > b > c > d$ ). Differences among water treatment stress using Kruskal–Wallis tests are denoted by asterisks (\*:  $P < 0.05$ ; \*\*:  $P < 0.01$ ; \*\*\*:  $P < 0.001$ ).



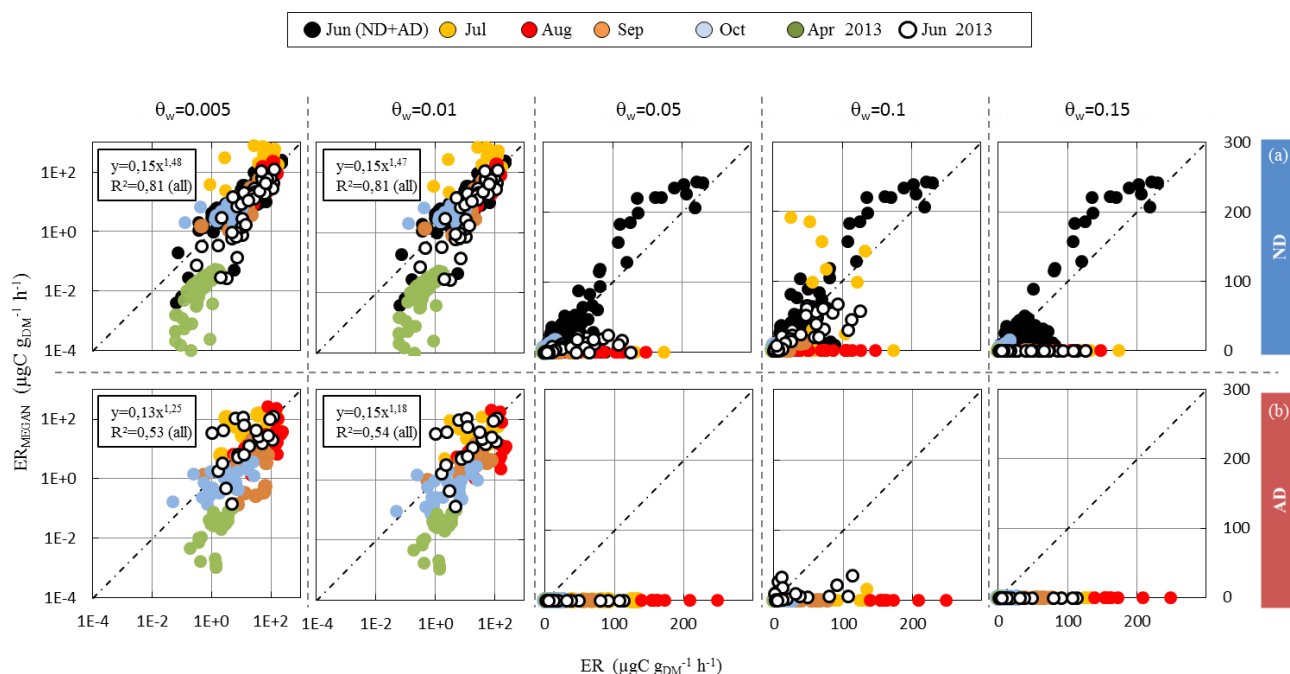


**Figure 3.** Comparison between isoprene emission rates (in  $\mu\text{gC g}_{\text{DM}}^{-1} \text{h}^{-1}$ ) calculated using MEGAN2.1 ( $\text{ER}_{\text{MEGAN}}$ , Guenther et al., 2012) and measured isoprene emission rates (ER) vs. the wilting point value  $\theta_w$  (0.005 to  $0.15 \text{ m}^3 \text{ m}^{-3}$ ), from June 2012 to June 2013, under (a) ND ( $n = 267$ ) and (b) AD ( $n = 138$ ). Since the rain exclusion device was only implemented soon prior to our study's commencement in June 2012, the ND and AD measurements were considered together for June 2012. Linear regressions for ND June 2012 were  $y = 1.13x - 12.05$ ,  $R^2 = 0.80$  ( $\theta_w = 0.05 \text{ m}^3 \text{ m}^{-3}$ );  $y = 1.13x - 7.13$ ,  $R^2 = 0.80$  ( $\theta_w = 0.1 \text{ m}^3 \text{ m}^{-3}$ ); and  $y = 1.12x - 16.94$ ,  $R^2 = 0.76$  ( $\theta_w = 0.15 \text{ m}^3 \text{ m}^{-3}$ ). The dotted line is the 1 : 1 line.

ER variability and sensitivity to drought observed during this study, we tested the latest version of the MEGAN model, which is widely used for air quality and climate change applications (MEGAN2.1, Guenther et al., 2012). In particular, the ability of its soil moisture coefficient activity  $\gamma_{\text{SM}}$  (Eq. 4a–c) to assess the observed effect of ND and AD treatments was examined over wilting point  $\theta_w$  values ranging from 0.01 to  $0.15 \text{ m}^3 \text{ m}^{-3}$ , which is representative of a large brand of soils (Ghanbarian-Alavijeh and Millán, 2009). Indeed, Müller et al. (2008) showed that isoprene assessments were very sensitive to  $\theta_w$ . For the record,  $\theta_w$  was  $0.15 \text{ m}^3 \text{ m}^{-3}$  at the  $\text{O}_3\text{HP}$ .

Assessed ( $\text{ER}_{\text{MEGAN}}$ ) and observed (ER) isoprene emission rates were compared separately for ND and AD. However, given that the rainout shelter was implemented close to the commencement of our study in June 2012, measurements carried out in the AD plot were not distinguished, only in the case of this month, from the ones taken in the ND plot (AD and ND data were thus mixed for June 2012).

For  $\theta_w < 0.05 \text{ m}^3 \text{ m}^{-3}$ , and regardless of the  $\theta_w$  value, MEGAN2.1 captured more than 80 % of the ER variability in the ND plot ( $y = 0.15x^{1.5}$ ,  $R^2 = 0.81$ , Fig. 3a), but less ( $\approx 50\%$ ) in the AD plot ( $R^2 = 0.53$  and  $0.54$  for  $\theta_w = 0.005$  and  $0.01 \text{ m}^3 \text{ m}^{-3}$  respectively, Fig. 3b). An overall overestimation of 25 % was associated with the MEGAN2.1 as-

essment for both treatments. On the contrary, for  $\theta_w \geq 0.05 \text{ m}^3 \text{ m}^{-3}$ , most of the isoprene emissions were set to zero by MEGAN2.1 in the AD plot, while in the ND only June observations were correctly assessed with an overall overestimation (regardless of the  $\theta_w$  values) of  $\approx 10\%$  ( $R^2$  ranging from 0.76 to 0.80 for  $\theta_w = 0.15$  and  $0.1 \text{ m}^3 \text{ m}^{-3}$  respectively). If some of the July  $\text{ER}_{\text{MEGAN}}$  were fairly close to the observations for  $\theta_w = 0.1 \text{ m}^3 \text{ m}^{-3}$ , the overall correlation was poor ( $y = 0.2x + 49.5$ ,  $R^2 = 0.02$ ).

Assuming that the discrepancies between  $\text{ER}_{\text{MEGAN}}$  and ER only resulted from the  $\gamma_{\text{SM}}$  formulation in MEGAN2.1 (and not from the other activity coefficients  $\gamma_{\text{P}}$ ,  $\gamma_{\text{T}}$ , or  $\gamma_{\text{A}}$  used, Eq. 3),  $\text{ER} / \text{ER}_{\text{MEGAN}}$  was calculated for both ND and AD treatments and was considered against the measured SW. In the ND treatment,  $\text{ER} / \text{ER}_{\text{MEGAN}}$  was not found to be significantly dependent on SW ( $y = 0.653e^{10.52x}$ ,  $R^2 = 0.13$ , Fig. 4a). However, in the AD plot,  $\text{ER} / \text{ER}_{\text{MEGAN}}$  increased exponentially with SW ( $y = 0.192e^{51.93x}$ ,  $R^2 = 0.66$ , Fig. 4b) and in particular when SW became higher than the wilting point  $\theta_w$  measured at the  $\text{O}_3\text{HP}$  site ( $0.15 \text{ m}^3 \text{ m}^{-3}$ ). Similar findings were obtained for SW-7, SW-14 and SW-21, for both the ND and AD treatments (Table 1).

In order to provide a better description of the impacts of ND and AD on ER as observed at the  $\text{O}_3\text{HP}$ , an empirical

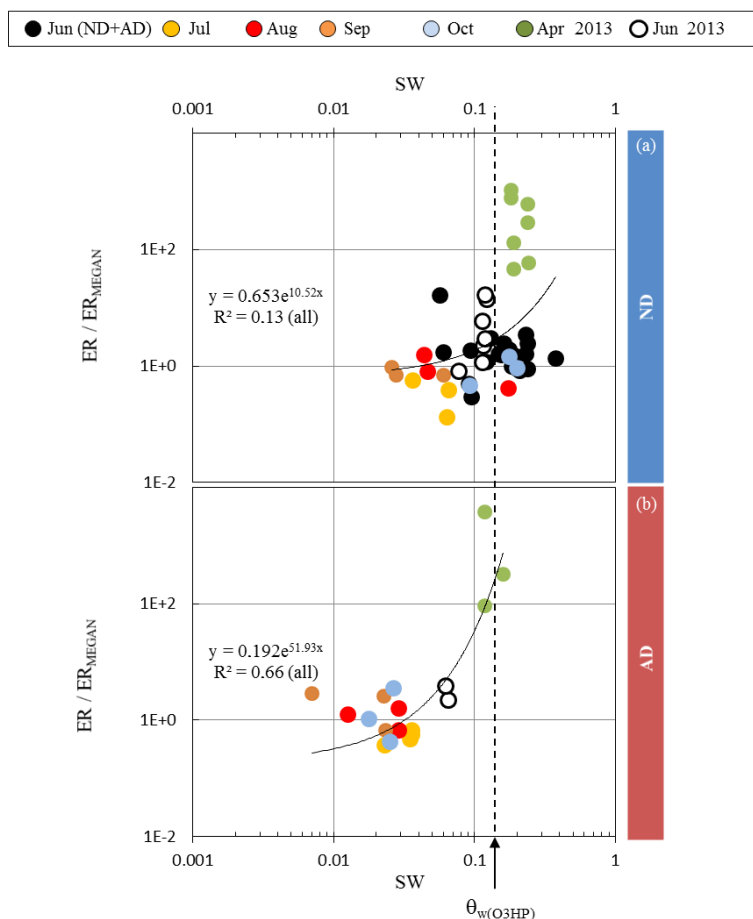


**Figure 4.** Ratio between observed (ER) and calculated ( $ER_{MEGAN}$ ) isoprene emission rates vs. the soil water content SW measured at the  $O_3HP$ , under (a) ND ( $n = 267$ ) and (b) AD ( $n = 138$ ). Given that the rain exclusion device was only implemented just before our study began in June 2012, the ND and AD measurements were considered together for June 2012. The dotted line is for  $SW = \theta_w$  measured at  $O_3HP$  ( $0.15 \text{ m}^3 \text{ m}^{-3}$ ).

type model, based on ANN optimisation of our observations at the  $O_3HP$ , was developed specifically for *Q. pubescens* isoprene emissions. Training and validation of the different ANNs tested were made using values of ER,  $T$ ,  $P$ , PAR, ST, and SW measured at the  $O_3HP$  (COOPERATE database). Environmental regressors  $x_i$  were integrated, using daily means, over a period ranging from 0 to 21 days prior to the measurements.

Among the different ANN settings tested, an optimised architecture,  $G_{14}$  (lowest RMSE between calculated and measured values, no overtraining, best correlation between measured and calculated ER over the whole range of value, see Boissard et al., 2008), was found for  $N = 3$  and a set of 16  $x_i$  with their corresponding connecting weights  $w_i$  (Appendix A). The final optimised RMSE (validation data) was  $8.5 \mu\text{gC g}_{DM}^{-1} \text{ h}^{-1}$ , for ER values ranging from 0.06 to  $113 \mu\text{gC g}_{DM}^{-1} \text{ h}^{-1}$ , and represents 35 % of the mean ( $22.7 \mu\text{gC g}_{DM}^{-1} \text{ h}^{-1}$ ). More than 80 % of the ER seasonal variations were assessed by  $G_{14}$ , regardless of the water treat-

ment (ND or AD) and the month, except in July (Fig. 5a), when ER variability was always poorly represented regardless of the different ANN settings considered. July corresponds to the period where trees started to adapt to ND and AD; this period was possibly insufficiently represented in our dataset to be well taken into account by our statistical approach. An overall underestimation of 6 % and 12 % was observed in the ND and AD respectively. For comparison,  $ER_{MEGAN}$  calculated with a value  $\theta_w$  of  $0.15 \text{ m}^3 \text{ m}^{-3}$  are presented again in Fig. 5b for both the ND and AD treatment.

Under ND, the global contribution of the two lowest frequencies ( $-14$  and  $-21$  days) considered in  $G_{14}$  was, relative to the contribution of the two highest frequencies (instantaneous and  $-7$  days), higher than under AD (Fig. 6). In particular, in October 2012 and April and June 2013, the two lowest frequencies respectively represented 20 %, 97 %, and 50 % of the total in the ND compared to 3 %, 55 %, and 26 % in the AD.

**Table 1.** Correlations between  $ER_{MEGAN}/ER$  and the soil water content (SW) cumulated over 7 to 21 days before the measurement.  $ER_{MEGAN}$  and  $ER$  are isoprene emission rates calculated using MEGAN2.1 (Guenther et al., 2012) and measured (this study) respectively.

$x$	ND		AD	
	$ER/ER_{MEGAN} = f(x)$	$R^2$ value	$ER/ER_{MEGAN} = f(x)$	$R^2$ value
SW	$0.653e^{10.5x}$	0.13	$0.192e^{51.1x}$	0.66
SW-7	$0.715e^{1.30x}$	0.13	$0.239e^{6.30x}$	0.55
SW-14	$0.763e^{0.57x}$	0.11	$0.279e^{2.74x}$	0.48
SW-21	$0.523e^{0.46x}$	0.14	$0.365e^{1.47x}$	0.38

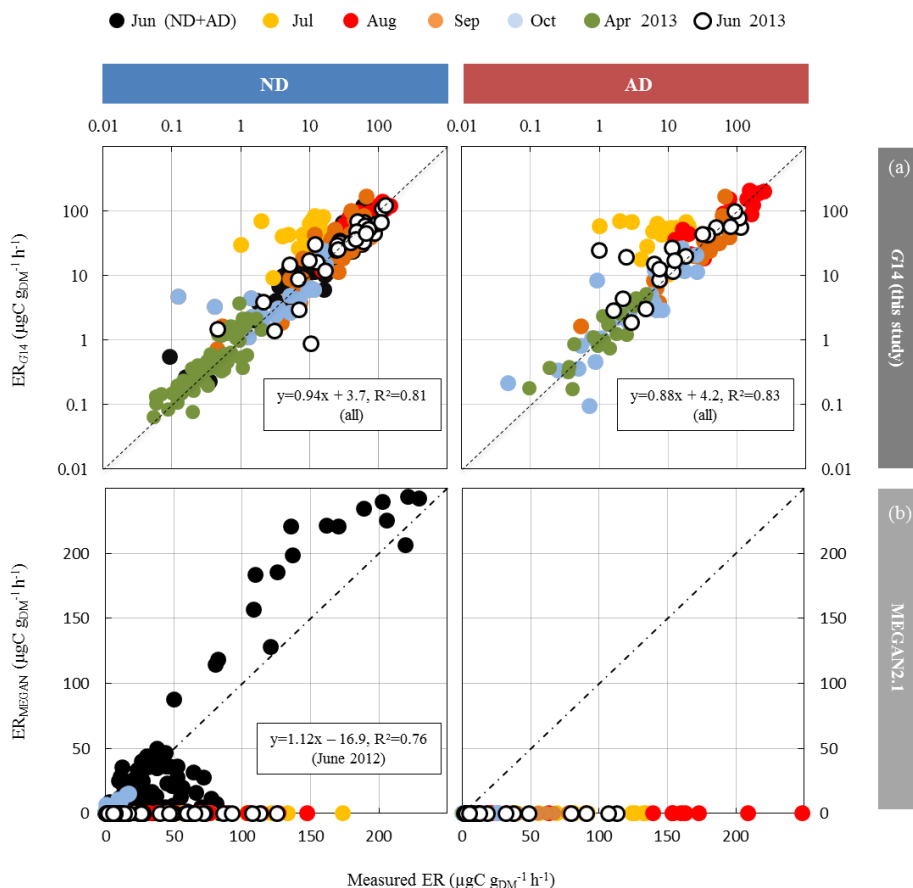


**Figure 5.** Calculated vs. measured isoprene emission rates (in  $\mu\text{gC g}_{\text{DM}}^{-1} \text{h}^{-1}$ ) under ND ( $n = 267$ ) and AD ( $n = 138$ ) from June 2012 to June 2013, using the (a) G14 (this study) and (b) MEGAN2.1 isoprene model (Guenther et al., 2012) with a wilting point value  $\theta_w$  of  $0.15 \text{ m}^3 \text{ m}^{-3}$  (measured at the  $\text{O}_3\text{HP}$ ). The dotted line is the 1 : 1 line.

### 3.4 ER sensitivity to expected climatic changes over the European Mediterranean area

Present and future  $T$ ,  $P$ , and PAR (ISI-MIP derived) as well as SW and ST (ORCHIDEE derived) were integrated over periods ranging from 0 to 21 days in order to be used in G14 and to assess  $ER_{G14}$  for present and future cases. Moderate (respectively severe) changes with regard to the present of SW,  $P$ , ST,  $T$ , and PAR were additionally calculated according to the RCP2.6 (respectively RCP8.5) scenario; however,

PAR relative changes were not considered as they were negligible for both moderate and severe scenarios.

Moderate changes of the environmental conditions (RCP2.6 scenario) implied a systematic positive monthly  $\Delta T$  throughout the year, whereas  $\Delta P$  was found to be positive only during the winter and negative during the summer (Fig. 7a). ST and SW changes were found to be in line with  $T$  and  $P$  respectively. The highest monthly relative changes were for  $P$  (+75 % in February and –30 % in July), whereas the smallest were for SW. Monthly ST and  $T$  relative changes

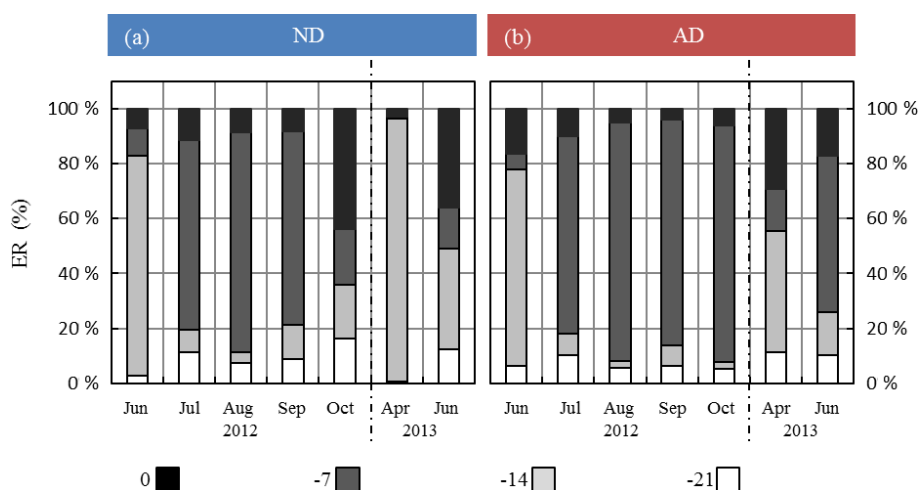


**Figure 6.** Seasonal variations of the relative contribution of the different frequencies as considered in  $G_{14}$  (0, 7, 14, and 21 days before the measurement) among the regressor  $x_i$  selected in  $G_{14}$ , under (a) ND ( $n = 267$ ) and (b) AD ( $n = 138$ ). The frequency “0”, “-7”, “-14”, “-21” includes the contribution of “ $L-1, T-1, SW-1, T_0, L_0, T_M-T_m$ ”; “ $SW-7, ST-7, P-7$ ”; “ $T-14, SW-14, ST-14, P-14$ ”; and “ $T-21, SW-21, P-21$ ” respectively.

**Table 2.** Annual absolute and relative changes to the present of SW,  $P$ , ST and  $T$  according to the RCP2.6 and RCP8.5 scenarios. Present and future cases were calculated for 2000–2010 and 2090–2100 respectively.

	$\Delta SW$ ( $m^3 m^{-3}$ )	$\Delta P_{cum}$ (mm)	$\Delta ST$ ( $^{\circ}C$ )	$\Delta T$	$\Delta SW / SW$	$\Delta P_{cum} / P_{cum}$ (%)	$\Delta ST / ST$	$\Delta T / T$
RCP2.6	+0.004	+30	+1.4	+1.4	+0.5	+5	+8.4	+9.1
RCP8.5	-0.007	+30	+5.3	+5.3	-5.0	-24	+32	+34

remained more or less constant (between +7 % and +10 %) between February and November. Overall,  $T$  and  $P_{cum}$  absolute (relative) annual changes were +1.4  $^{\circ}C$  and +34 mm respectively (+9.1 % and +4.8 % respectively, Table 2).

Under more severe environmental changes (RCP8.5 scenario), monthly  $T$  and ST increased all year round, whereas  $P$  and SW generally decreased, except in January, February, and November, when relative  $P$  changes were negligible (Fig. 7b). The annual absolute (relative) changes for  $T$  and  $P_{cum}$  were +5.3  $^{\circ}C$  and -124 mm respectively (+34 % and -24 % respectively, Table 2). In these conditions, the annual  $\Delta P_{cum} / P_{cum}$  was similar to the reduction experienced at the  $O_3HP$  during our study (-30 %). The highest monthly relative changes were found for ST: +96 % and +86 % in January and December respectively. During summertime the highest relative changes were found for  $P$  (-55 % and -62 % in July and August respectively).

$ER_{G14}$  was found to systematically increase compared to the present under  $T$  and  $TT$  changes, with an annual relative change of +80 % and +240 % respectively (Fig. 8a). The highest relative changes were noted in June and July. In contrast,  $ER_{G14}$  was almost not sensitive to  $P$  or  $PP$  changes, regardless of the month (annual relative change of +10 % and +8 % respectively, Fig. 8b). When the combined im-

pacts of changes in temperature and precipitation were considered,  $ER_{G14}$  was found to systematically increase all year round, following a seasonal trend that was extremely close to that found for the  $T$  and  $TT$  tests (Fig. 8c). However, the additional effect of the precipitation changes enhanced the increase noticed for temperature changes only: the annual increase was +100 % ( $T + P$ ) and +280 % ( $TT + PP$ ) compared to +80 % ( $T$ ) and +240 % ( $TT$ ). Note that the  $ER_{G14}$  seasonal trend calculated for the present did not match our observed  $ER$  variations. Indeed  $ER_{G14}$  was tuned using environmental parameters averaged over 24 h (and therefore integrated over the daytime and nighttime period), which were thus much lower than the environmental parameters measured during our daytime-only samplings (especially for PAR and  $T$ ).

## 4 Discussion

### 4.1 Impact of water stress on seasonal gas exchanges and isoprene emission of *Q. pubescens*

In spite of a significant  $G_w$  reduction in summer 2012 owing to the AD, *Q. pubescens* maintained a positive  $P_n$  during the summer, regardless of water stress (ND or AD). Electric resistivity tomography measurements carried out on the  $O_3HP$

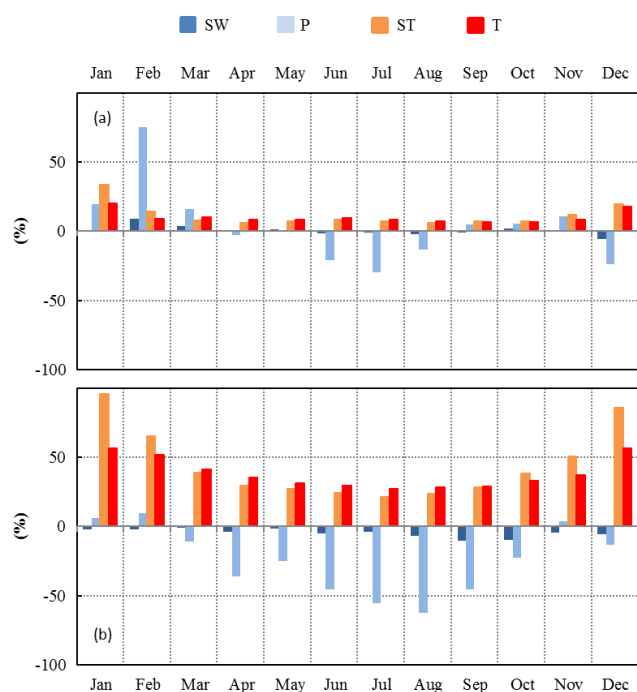


**Figure 7.** Seasonal variations between present (2000–2010) and future (2090–2100) relative changes of SW, P, ST, and T over the continental Mediterranean area obtained using (a) RCP2.6 and (b) RCP8.5 projections.

site revealed the heterogeneity of the karstic substrate, organised as soil pockets developed between limestone rocks. Water and nutrient pools and dynamics probably differed greatly between the shallow upper soil layers and the soil pockets developed between limestone rocks. However, the soil trenches in the site revealed that a calcareous slab often developed at a depth of 10–20 cm and that the roots of the oaks were often distributed in this humiferous horizon close to the surface, with very few roots crossing this slab. Water supply from layers deeper than 10–20 cm was thus not considered. Such behaviour enables trees to limit evapotranspiration under water stress, as a drought-acclimated species permits them to ensure sufficient accumulation of carbohydrates for the winter (Chaves et al., 2002). Such a strategy was also observed in a study conducted on the same species but under greenhouse conditions (Genard-Zielinski et al., 2015). The seasonal regulation and conservation of  $P_n$  and  $G_w$  enabled isoprene emissions to be maintained even during the summer water stress (ND and AD).

The maximum  $\varepsilon_{\text{iso,Qp}}$  in both plots was close to previously measured values obtained for the same species under Mediterranean conditions during greenhouse and in situ experiments (114.3 and 134.7  $\mu\text{gC g}_{\text{DM}}^{-1} \text{h}^{-1}$ ) by Genard-Zielinski et al. (2015) and Simon et al. (2005) respectively. The difference observed in April 2013 between  $\varepsilon_{\text{iso,Qp}}$  in the ND and AD could not be attributed solely to the AD effect. Indeed, apart from a possible “memory effect” of the AD

applied during 2012, the observed difference was probably due to the high natural variability in bud breaking and isoprene emission onset at this point of the year. The observed significant increase (a factor of 2) in  $\varepsilon_{\text{iso,Qp}}$  under AD (August and September) illustrates how isoprene is likely to be important for short-term *Q. pubescens* drought resistance, in particular through the ability of isoprene to stabilise the thylakoids membrane, under (for example) thermal or oxidative stress (Peñuelas et al., 2005; Velikova et al., 2012). Moreover, previous studies have highlighted the possibility for a plant growing under water stress to synthesise isoprene using an alternative carbon source (extra-chloroplastic carbohydrates) (Lichtenthaler et al., 1997; Funk et al., 2004; Brillì et al., 2007). For species emitting other BVOCs than isoprene, but studied in the Mediterranean area under water stress, Lavoit et al. (2009) reported lower (a factor of  $\approx 2$ ) monoterpene emission rates from *Quercus ilex* under AD from June to August, during the second and third year of rain exclusion. Since *Q. ilex* does not possess specific leaf reservoirs for monoterpene storage, *Q. ilex* monoterpene emissions are hence de novo and their emissions are tightly related to their synthesis according to light and temperature as isoprene.

The significant uncoupling between ER and  $C_L \times C_T$  reported for the July measurements occurred when SW significantly decreased to their seasonal minimum values (0.05 and 0.03  $\text{m}^3 \text{m}^{-3}$ ) at the O<sub>3</sub>HP in both plots. A similar uncoupling has also been observed for some other strong isoprene emitters under water stress (*Quercus serrata* and *Quercus crispula*, Tani et al., 2011). These findings may confirm these authors’ assumptions that extra-chloroplastic isoprene precursors supply the carbon basis for isoprene biosynthesis (and not only from CO<sub>2</sub> fixed instantaneously in the chloroplast) when water stress occurs, which explains why isoprene emissions become less dependent on the classical abiotic factors PAR and T as considered by Guenther et al. (1995).

#### 4.2 Improving consideration of the drought effect in isoprene emission models

Since ND and AD conditions tested by *Q. pubescens* in our study stood aside from optimal growth conditions under which empirical emission models perform fairly well, it was interesting to test the ability of MEGAN2.1 to reproduce the observed impacts of a water deficit, as in O<sub>3</sub>HP, on isoprene emissions. The formulation of the MEGAN2.1 soil moisture factor  $\gamma_{\text{SM}}$ , wilting point centred, was deemed inadequate for reproducing the observed isoprene variability of a drought-adapted emitter such as *Q. pubescens*. Thus, MEGAN2.1 very successfully reproduced observed ER variability under the ND (more than 80 %) only when  $\gamma_{\text{SM}}$  was not operating; in fact, only when very low values of the wilting point were selected ( $\theta_w \leq 0.01 \text{ m}^3 \text{m}^{-3}$ ),  $\gamma_{\text{SM}}$  was set to 1. In practice, wilting point values lower than 0.01  $\text{m}^3 \text{m}^{-3}$  are encountered very rarely, and only for loamy sand soils

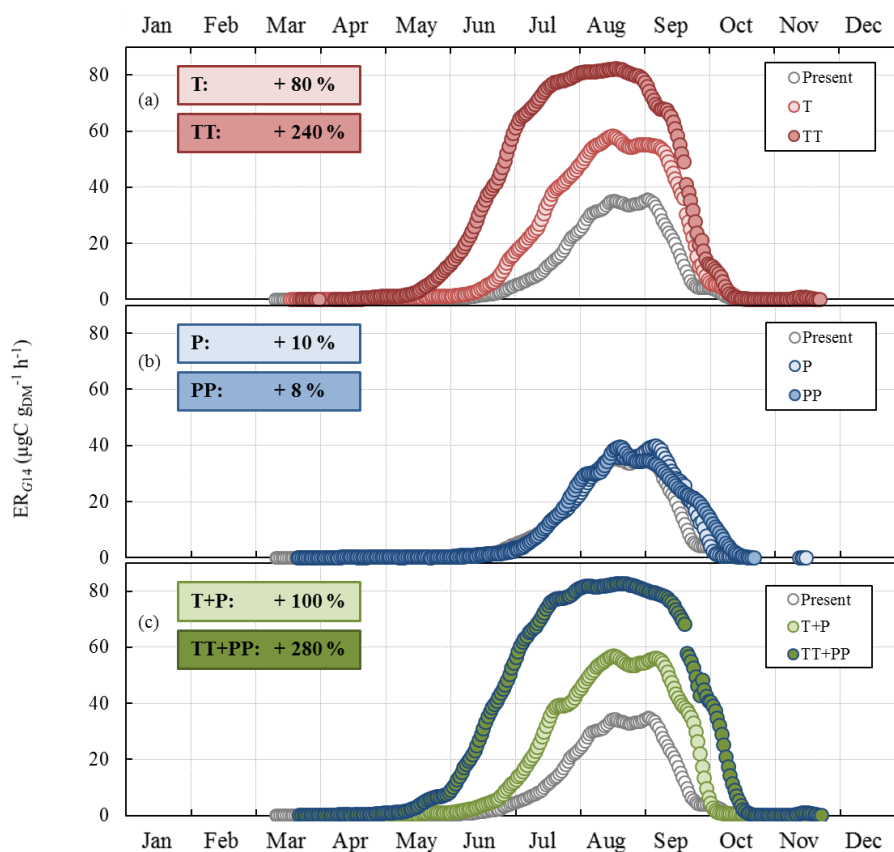


**Figure 8.** Sensitivity of the seasonal variation of isoprene emission rates calculated using  $G14$  ( $ER_{G14}$ , in  $\mu\text{gC g}_{\text{DM}}^{-1} \text{h}^{-1}$ , this study) to (a)  $T$  and  $ST$  changes as in RCP2.6 ( $T$  case) and RCP8.5 ( $TT$  case) respectively; (b)  $SW$  and  $P$  changes as in RCP2.6 ( $P$  case) and RCP8.5 ( $PP$  case) respectively; and (c) combined  $T$ ,  $ST$ ,  $P$ , and  $SW$  changes as in RCP2.6 ( $T+P$  case) and RCP8.5 ( $TT+PP$  case) respectively. Present and future cases were calculated for 2000–2010 and 2090–2100 respectively. Overall annual relative changes to present are framed.

(Ghanbarian-Alavijeh and Millán, 2009), and so did not apply in the case of *Q. pubescens* in the present study. Once higher  $\theta_w$  values ( $\geq 0.05 \text{ m}^3 \text{ m}^{-3}$ ) were tested,  $\gamma_{\text{SM}}$ , and with it almost all the isoprene emissions, rapidly decreased to zero once the drought was underway (i.e., after the June measurements). On a larger scale (over subtropical Africa), Müller et al. (2008) found that MEGAN underestimation of isoprene emissions was also the largest after the drought was reached. Consequently, for a drought-adapted isoprene emitter, not only was the wilting point not found to be a relevant parameter to be considered in the expression of  $\gamma_{\text{SM}}$ , but also a formulation that could stop isoprene emissions, regardless of the drought intensity.

The fact that under ND the discrepancies between  $ER_{\text{MEGAN}}$  and  $ER$  were not found to be contingent on the soil water content  $SW$  (Fig. 4a) illustrates that under a natural drought intensity the capacity of a drought-resistant species to emit isoprene, that is to trigger physiological regulations to protect its cellular structures, is primarily due to its natural adaptation, and not to the water available in the soil. Isoprene emissions became  $SW$  dependent only when the adaptation of *Q. pubescens* to its “natural” environment was threatened

(i.e., the AD treatment, Fig. 4b). Thus, for a species that is not adapted to drought, such as *Populus deltoides*, the appearance of unusual water stress conditions would strongly affect and limit its isoprene emissions, as previously reported by Pegoraro et al. (2004). Indeed, this reference is the only one used by Guenther et al. (2006) to account for the impact of the soil water content in MEGAN2.1; the  $\gamma_{\text{SM}}$  factor cannot effectively account for isoprene emission variability for drought-adapted emitters such as *Q. pubescens*. Such a discrepancy under conditions other than Mediterranean was also noticed by Potosnak et al. (2014) during a seasonal study over a mixed broad-leaf forest primarily composed of *Q. alba* L. and *Q. velutina* Lam. (Missouri, USA). Guenther et al. (2013) have suggested that including the soil moisture averaged over longer periods of time (such as the previous month and not only the mean over the previous 240 h) may help to improve predictions during drought periods. In this study we found that the discrepancies between  $ER_{\text{MEGAN}}$  and  $ER$  were not related to the frequency over which  $SW$  was considered (Table 1): under ND they remained  $SW$  independent, whereas under AD the correlation between  $ER / ER_{\text{MEGAN}}$  and  $SW$  remained of the same

order ( $0.66 \leq R^2 \leq 0.38$ ) but with a best fit found for the soil water content of the current day. These findings suggest that the formulation of the soil moisture activity factor could be improved in MEGAN2.1 if at least two distinct types of isoprene emitters were considered: (i) non-drought-adapted species (such as *Populus deltoides*) from which isoprene emissions would be modulated using the actual  $\gamma_{SM}$  formulation and (ii) drought-adapted emitters (such as *Q. pubescens*), for which  $\gamma_{SM}$  would modulate isoprene emissions relative to SW, without diminishing them to zero, in an exponential way similar to the expression found in this study,  $\gamma_{SM} = 0.192e^{51.93 SW}$  (see Sect. 3.3). However, validation of such an expression to other drought-adapted isoprene emitters, as well as to other drought-adapted BVOC emitters, is required and will necessitate further field and controlled ad hoc experiments.

Moreover, the largest discrepancies between  $ER_{MEGAN}$  and ER were noticed for the measurements in April and for some of those in June (Figs. 3 and 4), i.e., in periods when the drought (whether natural or amplified) was yet to be completely underway during our study. This highlights that ER variability during the onset and seasonal increase in isoprene emissions was not solely drought or SW dependent, even in a water-limited environment such as the O<sub>3</sub>HP. Indeed, as observed for *Q. alba* and *Q. macrocarpa* Michx, the isoprene onset was found to be strongly correlated with ambient temperature cumulated over  $\approx 2$  weeks (200 to 300 degree day, Dd, °C), while the maximum ER was observed at 600–700 Dd °C (respectively Geron et al., 2000 and Petron et al., 2001). However, if part of this dynamical regulation is already included in MEGAN2.1 through its emission activity factors  $\gamma_T$  and  $\gamma_A$  (see Eq. 3), the combined effect of temperature regulation and drought is not fully accounted for. For instance, Wiberley et al. (2005) observed that the onset of kudzu isoprene emissions was shortened by 1 week under elevated temperature compared to cold growth.  $ER_{G14}$  consequently became more sensitive to rapid environmental changes as drought intensity increased: the overall averaged relative contributions of the regressors  $x_i$  cumulated over 14 and 21 days decreased by 45 % and 29 % in the ND and AD respectively. Interestingly, these changes were found to be highest during the months of October 2012 (35 % and 8 % in the ND and AD respectively), April 2013 (from 96 % to 55 % in the ND and AD respectively), and June 2013 (49 % and 26 % in the ND and AD respectively, Fig. 6). Therefore, during the senescence and onset periods, the drought affected the dynamical regulation of isoprene emission more than the emissions themselves. Thus, an ANN approach as used in this study to develop G14 highlights the importance of including a modulation along the season of the range of frequencies over which the relevant environment regressors should be considered.

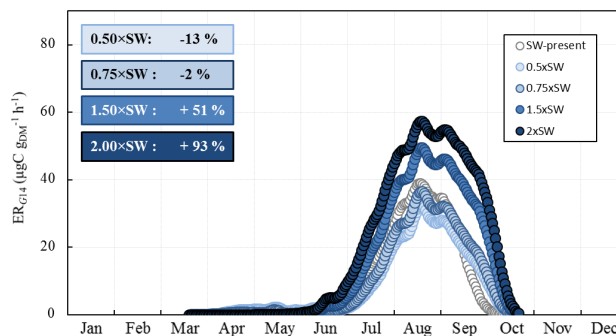


**Figure 9.** Sensitivity of the seasonal variation of isoprene emission rates calculated using G14 ( $ER_{G14}$ , in  $\mu\text{gC}_{\text{gDM}}^{-1} \text{h}^{-1}$ ) to SW. Overall annual relative changes to present (2000–2010) are framed.

### 4.3 How will climatic changes affect the seasonal variations of *Q. pubescens* isoprene emissions in the Mediterranean area?

In the future, the Mediterranean area investigated in this study will face changes in terms of precipitation regime (thus of soil water content) and/or changes in ambient temperature (thus of soil temperature). Depending on the CO<sub>2</sub> trajectory scenario considered, the annual  $P_{\text{cum}}$  would remain more or less stable (RCP2.6), or decrease by 24 % (RCP8.5); however, the seasonal regime would change, with a summer reduction of  $P$  in both cases. The O<sub>3</sub>HP experimental strategy used in this work illustrates the upper limit of the drought intensity that *Q. pubescens* could undergo by 2100 in the Mediterranean area. On the other hand, temperature would increase regardless of the scenario and month, from 1.4 (+10 %) to 5.3 °C (+34 %) annually.

As expected,  $ER_{G14}$  was found to increase appreciably with temperature increase, from 80 % annually in the RCP2.6 scenario to 240 % in RCP8.5 (Fig. 8a). If such an increase is generally estimated and observed when considering a range of temperature enhancements that accord with future projected changes (Peñuelas and Staudt, 2010), such a response seems fairly unclear under Mediterranean water deficit conditions (Llusià et al., 2008, 2009). On a global scale, Müller et al. (2008) estimated a 20 % decrease in isoprene due to soil water stress. In our case, isoprene emissions were found to be scarcely sensitive to  $P$ , regardless of the intensity of changes: at most, annual  $P$  would increase isoprene emissions by 10 %, regardless of the intensity of  $P$  changes investigated over the scenario considered (Fig. 8b). This finding is in line with our observations: except in October 2012, monthly averaged ER were not significantly different in the ND and the AD (Fig. 2c). However, if the observed SW did differ between the ND and the AD plots ( $\approx$  a factor of 2, Fig. 1), SW calculated by the ORCHIDEE model was almost entirely unaffected by the  $P$  changes, even in the severe scenario RCP8.5. Such an uncoupling between  $P$  and SW could be explained by modifications in the ORCHIDEE

model of the overall soil water evapotranspiration, runoff, and drainage which in short lead to near-constant SW values. In order to test the impact of the sole SW changes within a similar range to that observed at the O<sub>3</sub>HP between ND and AD, ER<sub>G14</sub> seasonal variation was calculated using present SW multiplied every day by 0.5, 0.75, 1.5, and 2 (Fig. 9). Surprisingly, ER<sub>G14</sub> was almost unchanged when SW was reduced (−2% and −13% annually for 0.5 × SW and 0.75 × SW respectively). ER<sub>G14</sub> increased only when SW increased: +51% and +93% annually for 1.5 × SW and 2 × SW respectively. These results are in line with our findings that, under a certain level of SW, isoprene emissions from a drought-adapted emitter such as *Q. pubescens* are no more affected by soil water content. Indeed, under ND, ER / ER<sub>MEGAN</sub> was not correlated with SW, but, under AD, ER / ER<sub>MEGAN</sub> remained more or less stable when SW was lower than the wilting point (Fig. 4 and Sect. 3.3). Isoprene emission variations would be highly SW dependent only for the highest SW values: (i) in the spring and in the beginning of the summer when the drought is not completely underway and (ii) in the fall when the drought stress is fading away and when the highest differences are assessed between ER<sub>G14</sub> calculated for SW-present and for 2 × SW (Fig. 9). When the *T* and *P* effects were combined, the seasonal variation of ER<sub>G14</sub> was affected in a similar way to when the sole *T* effect was considered, but with an enhanced increase: +20% and +40% between *T* and *T*+*P* tests, and between the *T* + *P* and *TT* + *PP* tests respectively (Fig. 8a, c). Such higher sensitivity of *Q. pubescens* isoprene emissions to temperature stress under drought was also observed by Genard-Zielinski (2014). Understandably, the *G*14 algorithm developed in this study to assess isoprene emissions in future climates should be validated through a longer period of measurement, in order to assess how *Q. pubescens* acclimates over a more extensive period of drought and to confirm or deny these findings. In this context, measurements have been carried out at the O<sub>3</sub>HP on the same branches as the ones studied in this work since June 2013 (Saunier et al., 2017).

These findings were attained considering an unchanged *Q. pubescens* biomass, i.e., unaffected by long-term acclimation to *T* and drought increase. However, one can question whether *Q. pubescens* could maintain such a high allocation of its primary assimilated carbon (primary plant metabolites) to isoprene emissions (secondary plant metabolites). Indeed, Genard-Zielinski et al. (2015) have shown that under moderate and severe drought, *Q. pubescens*' aerial and foliar growth is negatively affected. Thus, in the long term, such a cost of drought could affect the overall energy budget and expedite plant senescence (Loreto and Schnitzler, 2010). The assessed ER<sub>G14</sub> increase could then be offset or even reversed.

On the other hand, one should also consider the additional co-effects of the CO<sub>2</sub> increase expected in the future. Bytnerowicz et al. (2007) have reported that if temperature increase proves to have little effect, elevated CO<sub>2</sub> would favour

both the growth and water use efficiency of plants and account for a 15%–20% increase in forest NPP (net primary production). When CO<sub>2</sub> enhancement was considered, the leaf mass per square metre of the PFT tested in ORCHIDEE in this study (broad-leaf temperate) was predicted to undergo a relative increase by 35% and 100% under RCP2.6 and RCP8.5 respectively. Tognetti et al. (1998) observed a similar positive effect on the assimilation rate of both *Q. pubescens* and *Q. ilex* during a long-term CO<sub>2</sub> enhancement study and measured a net increase in the diurnal course of isoprene emissions. Thus, the major impact of future climate change on isoprene emissions could eventually be related to a general change in land cover, with Mediterranean species shifting to more favourable conditions.

## 5 Conclusion

The study carried out in 2012–2013 at the O<sub>3</sub>HP on *Q. pubescens* was the first to test *in natura* and on a seasonal scale the effects of drought (ND and AD) on gas exchange, and in particular isoprene emissions of a mature copice. This unique set of experimental data has confirmed how a drought-adapted species was able (i) to limit its evapotranspiration under water stress, even in summer, in order to maintain a similar level of net assimilation regardless of the drought intensity and (ii) to emit similar or even higher amounts of isoprene in order to protect cellular structures under drought (ND or AD) episodes. In an environment such as the O<sub>3</sub>HP (elevated ambient temperature and scarcity of the water available), and for a drought-adapted emitter such as *Q. pubescens*, isoprene emissions were thus maintained, and in the ND their variability was not dependent on the soil water content. However, under the AD treatment, isoprene emissions were found to exponentially decrease with SW, in particular when SW was lower than the wilting point measured at the site ( $\theta_w = 0.15 \text{ m}^3 \text{ m}^{-3}$ ).

Since the intensity of isoprene emissions in the Mediterranean area is large, and can occur together and close to large urban emissions of other reactive compounds (in particular NO<sub>x</sub> emissions), the impacts of future environmental changes on isoprene emissions in this area need to be assessed as precisely as possible. The latest version of the empirical isoprene model, MEGAN2.1, was found to be unable to reproduce the effect of drought on isoprene emissions from *Q. pubescens*, regardless of the drought intensity (ND or AD). However, for such a drought-adapted emitter, MEGAN2.1 performed very well in capturing the seasonal ER variability (more than 80%) under ND when its soil moisture activity factor  $\gamma_{SM}$  was not operating ( $\gamma_{SM} = 1$ ); this performance decreased to  $\approx 50\%$  in the AD treatment. We suggest that, in addition to the actual  $\gamma_{SM}$  expression, which is only valid for non-drought-adapted emitters, a specific formulation should be considered for drought-adapted emitters involving an exponential decrease in isoprene emis-



sion with SW decreasing to above-zero values, as proposed in this study for *Q. pubescens*. An ANN approach similar to that undertaken to develop *G14* highlighted its ability to extract from appropriate field data measurements the relevant environmental regressors to be considered and the relevant frequency over which they should be employed. *G14* was able to reproduce more than 80 % of the ER seasonal variability observed for *Q. pubescens*, regardless of the drought intensity. Moreover, the application of *G14* to future climate environmental data derived from IPCC RCP2.6 and RCP8.5

scenarios suggests that isoprene emissions in the future will be mainly affected by warmer conditions (up to an annual 240 % increase for the most severe warming scenario), not by drier conditions (at most, a 10 % increase annually). The major impact of amplified drought will actually consist of enhancing (by up to 40 %) the sensitivity of isoprene emissions to thermal stress.

*Data availability.* If requested, data will be kindly provided by contacting the correspondence author.

**Appendix A: Calculation of isoprene emission rates  $ER_{G14}$  ( $\mu\text{gC g}_{\text{DM}}^{-1} \text{h}^{-1}$ ) using the G14 algorithm**

Due to the large range of ER variations, emissions were considered as logER, where

$\log ER_{G14} = \log[ER_{G14(\text{CN})}] \times s + m$  and  $s$  is the standard deviation of  $\log ER_{G14}$  ( $s = 0.8916$ ),  $m$  is the mean of  $\log ER_{G14}$  ( $m = 0.8434$ ), and  $\log[ER_{G14(\text{CN})}]$  is the central-normalised log10 of  $ER_{G14}$  calculated as

$$\log[ER_{G14(\text{CN})}] = w_0 + w_{1,k} \times \tanh(N_1) + w_{2,k} \times \tanh(N_2) + w_{3,k} \times \tanh(N_3),$$

where

$$N_1 = w_{0,1} + \sum_{i=1}^{i=16} \sum_{j=1}^{j=16} w_{i,1} \times x_j,$$

$$N_2 = w_{0,2} + \sum_{i=1}^{i=16} \sum_{j=1}^{j=16} w_{i,2} \times x_j,$$

$$N_3 = w_{0,3} + \sum_{i=1}^{i=16} \sum_{j=1}^{j=16} w_{i,3} \times x_j.$$

**Table A2.** The selected input regressors  $x_i$ .

$x_1$	L0
$x_2$	L-1
$x_3$	T0
$x_4$	T-1
$x_5$	$T_M - T_m$
$x_6$	T-14
$x_7$	T-21
$x_8$	SW-1
$x_9$	SW-7
$x_{10}$	SW-14
$x_{11}$	SW-21
$x_{12}$	ST-7
$x_{13}$	ST-14
$x_{14}$	P-7
$x_{15}$	P-14
$x_{16}$	P-21

**Table A1.** The optimised weights  $w$ .

$w_0$	-1.29837907				
$w_{0,1}$	-0.16226148	$w_{0,2}$	2.90404784	$w_{0,3}$	0.23868843
$w_{1,1}$	0.07736039	$w_{1,2}$	2.18450515	$w_{1,3}$	-0.1283214
$w_{2,1}$	0.04806346	$w_{2,2}$	-0.0074737	$w_{2,3}$	0.06711214
$w_{3,1}$	-0.32907201	$w_{3,2}$	0.31067189	$w_{3,3}$	0.14496404
$w_{4,1}$	0.54847219	$w_{4,2}$	0.40895098	$w_{4,3}$	-1.1895104
$w_{5,1}$	-0.03820985	$w_{5,2}$	0.27886813	$w_{5,3}$	0.35561345
$w_{6,1}$	0.34677986	$w_{6,2}$	0.2906721	$w_{6,3}$	-2.84020867
$w_{7,1}$	-1.44104866	$w_{7,2}$	-1.23651445	$w_{7,3}$	4.30350692
$w_{8,1}$	-0.63559865	$w_{8,2}$	-0.63879809	$w_{8,3}$	3.61172683
$w_{9,1}$	0.81398482	$w_{9,2}$	0.85053882	$w_{9,3}$	0.46501183
$w_{10,1}$	-2.01376339	$w_{10,2}$	1.59664603	$w_{10,3}$	-0.74513053
$w_{11,1}$	1.61737626	$w_{11,2}$	-1.68773125	$w_{11,3}$	-2.29893094
$w_{12,1}$	-0.57093409	$w_{12,2}$	-0.76488022	$w_{12,3}$	1.96571085
$w_{13,1}$	0.78483127	$w_{13,2}$	0.9786783	$w_{13,3}$	-1.88733755
$w_{14,1}$	0.05311514	$w_{14,2}$	-0.88244467	$w_{14,3}$	-1.90110521
$w_{15,1}$	-0.47856411	$w_{15,2}$	-0.88883049	$w_{15,3}$	1.35713546
$w_{16,1}$	0.39618491	$w_{16,2}$	0.55564983	$w_{16,3}$	-0.73830992
$w_{1,k}$	-2.22601227	$w_{2,k}$	-1.64346181	$w_{3,k}$	-1.32117586

**Author contributions.** ACGZ, CB, EO, JL, JPO, BTR, and CF participated in the field experiments. ACGZ and CB processed the experimental, neural network, and MEGAN 2.1 data; CB processed the isoprene sensitivity tests for future climate changes. SB and BG performed the ORCHIDEE simulations. IMR managed and provided the COOPERATE environmental data. CB wrote the manuscript with the support of ACGZ, JL, CF, EO, IMR, BTR, and all other authors. Figures and tables were produced by ACGZ and CB. All authors commented on the manuscript.

**Competing interests.** The authors declare that they have no conflict of interest.

**Acknowledgements.** We are particularly grateful to Pierre Eric Blanc, Jean Claude Brunel, Gérard Castagnoli, Armand Rotereau, and other OHP staff for support before and during the different campaigns. We thank members of the DFME team from IMBE: Stéphane Greff, Caroline Lecareux, Sylvie Dupouyet, and Anne Bousquet-Melou for their help during measurements and analysis. This work was supported by the French National Agency for Research (ANR) through the projects CANOPÉE (ANR-2010 JCJC 603 01) and SecPriMe<sup>2</sup> (ANR-12-BSV7-0016-01), INSU (ChARMEx), CNRS National program EC2CO-BIOEFFECT (ICRAM project), and CEA. We are grateful to ADEME/PACA for PhD funding. For O<sub>3</sub>HP facilities, the authors thank the research federation ECCOREV FR3098 and the LABEX OT-Med (no. ANR-11-LABEX-0061), funded by the French Government through the A\*MIDEX project (no. ANR-11-IDEX-0001-02). The authors thank the MASSALYA instrumental platform (Aix Marseille Université, [lce.univ-amu.fr](http://lce.univ-amu.fr)) for the analysis and measurements used in this publication.

Edited by: Xinming Wang

Reviewed by: four anonymous referees

## References

- Affek, H. P. and Yakir, D.: Natural abundance carbon isotope composition of isoprene reflects incomplete coupling between isoprene synthesis and photosynthetic carbon flow, *Plant Physiol.*, 131, 1727–1736, 2003.
- Ashworth, K., Boissard, C., Folberth, G., Lathièrre, J., and Schurgers, G.: Global modelling of volatile organic compound emissions, in: *Biology, Controls and Models of Tree Volatile Organic Compound Emissions*, edited by: Niinemets, Ü., Monson, R. K., Springer Science + Business Media, Dordrecht, the Netherlands, *Tree Physiol.*, 5, 451–487, 2013.
- Atkinson, R. and Arey, J.: Atmospheric chemistry of biogenic organic compounds, *Acc. Chem. Res.*, 31, 9, 574–583, <https://doi.org/10.1021/ar970143z>, 1998.
- Atkinson, R. and Arey, J.: Gas phase tropospheric chemistry of biogenic volatile organic compounds: a review, *Atmos. Environ.*, 37, 197–219, 2003.
- Bishop, C. M.: *Neural networks for pattern recognition*, Oxford University Press, Oxford, UK, 504 pp., 1995.
- Boissard, C., Chervier, F., and Dutot, A. L.: Assessment of high (diurnal) to low (seasonal) frequency variations of isoprene emission rates using a neural network approach, *Atmos. Chem. Phys.*, 8, 2089–2101, <https://doi.org/10.5194/acp-8-2089-2008>, 2008.
- Brilli, F., Barta, C., Fortunati, A., Lerdau, M., Loreto, F., and Centritto M.: Response of isoprene emission and carbon metabolism to drought in white poplar (*Populus alba*) saplings, *New Phytol.*, 175, 244–254, 2007.
- Brüggemann, N. and Schnitzler, J.: Comparison of isoprene emission, intercellular isoprene concentration and photosynthetic performance in water-limited oak (*Quercus pubescens* Willd. and *Quercus robur* L.) saplings, *Plant Biol.*, 4, 456–463, 2002.
- Bytnerowicz, A., Omasa, K., and Paoletti, E.: Integrated effects of air pollution and climate change on forests: A northern hemisphere perspective, *Environ. Pollut.*, 147, 438–445, 2007.
- Calfapietra, C., Fares, S., and Loreto, F.: Volatile organic compounds from Italian vegetation and their interaction with ozone, *Environ. Pollut.*, 157, 1478–1486, 2009.
- Cappellin, L., Karl, T., Probst, M., Ismailova, O., Winkler, P. M., Soukoulis, C., Aprea, E., Maerk, T. D., Gasperi, F., and Biasoli, F.: On quantitative determination of volatile organic compound concentrations using Proton Transfer Reaction Time-of-Flight Mass Spectrometry, *Environ. Sci. Technol.*, 46, 2283–2290, 2012.
- Chameides, W. L., Lindsay, R. W., Richardson, J., and Kiang, C. S.: The role of biogenic hydrocarbons in urban photochemical smog – Atlanta as a case-study, *Science*, 241, 1473–1475, 1988.
- Chaves, M. M., Pereira, J. S., Maroco, J., Rodrigues, M. L., Ricardo, C. P. P., Osorio, M. L., Carvalho, I., Faria, T., and Pinheiro, C.: How plants cope with water stress in the field. Photosynthesis and growth, *Ann. Bot.*, 89, 907–916, 2002.
- Chaxel, E. and Chollet, J. P.: Ozone production from Grenoble city during the August 2003 heatwave, *Atmos. Environ.*, 43, 4784–4792, 2009.
- Chen, F. and Dudhia, J.: Coupling an advanced land surface-hydrology model with the Penn State-NCAR MM5 modeling system, Part I: Model implementation and sensitivity, *Mon. Weather Rev.*, 129, 569–585, 2001.
- Curci, G., Beekmann, M., Vautard, R., Siamek, G., Steinbrecher, R., Theloke, J., and Friedrich, R.: Modeling study of the impact of isoprene and terpene biogenic emissions on European ozone levels, *Atmos. Environ.*, 43, 1444–1455, 2009.
- Dreyfus, G., Martinez, J.-M., Samuelides, M., and Thiria, S.: *Réseaux de neurones: Méthodologies et Applications*, Eyrolles, France, 386 pp., 2002.
- Funk, J. L., Mak, J. E., and Lerdau, M. T.: Stress-induced changes in carbon sources for isoprene production in *Populus deltoides*, *Plant Cell Environ.*, 27, 747–755, 2004.
- Genard-Zielinski, A. C., Ormeño, E., Boissard, C., and Fernandez, C.: Isoprene emissions from Downy Oak under water limitation during an entire growing season: what cost for growth?, *PLoS ONE*, 9, e112418, <https://doi.org/10.1371/journal.pone.0112418>, 2014.
- Genard-Zielinski, A.-C., Boissard, C., Fernandez, C., Kalogridis, C., Lathièrre, J., Gros, V., Bonnaire, N., and Ormeño, E.: Variability of BVOC emissions from a Mediterranean mixed forest in southern France with a focus on *Quercus pubescens*, *Atmos. Chem. Phys.*, 15, 431–446, <https://doi.org/10.5194/acp-15-431-2015>, 2015.

- Geron, C., Guenther, A. B., Sharkey, T., and Arnts, R. R.: Temporal variability in basal isoprene emission factor, *Tree Physiol.*, 20, 799–805, 2000.
- Ghanbarian-Alavijeh, B. and Millán, H.: The relationship between surface fractal dimension and soil water content at permanent wilting point, *Geoderma*, 151, 224–232, <https://doi.org/10.1016/j.geoderma.2009.04.014>, 2009.
- Giorgi, F. and Lionello, P.: Climate change projections for the Mediterranean region, *Global Planet. Change*, 63, 90–104, 2008.
- Goldstein, A. and Steiner, A. H.: Biogenic VOCs, in: *Volatile Organic Compounds in the Atmosphere*, edited by: Koppmann R., Blackwell Publishing Ltd, Oxford, UK, 82–128, 2007.
- Grote, R., Morfopoulos, C., Niinemets, U., Sun, Z., Keenan, T. F., Pacifico, F., and Butler, T.: A fully integrated isoprenoid emissions model coupling emissions to photosynthetic characteristics, *Plant Cell Environ.*, 37, 1965–1980, 2014.
- Guenther, A. B., Hewitt, C. N., and Erickson, D., Fall, R., Geron, C., Graedel, T., Harley, P., Klinger, L., Lerdau, M., McKay, W. A., Pierce, T., Scholes, B., Steinbrecher, R., Tallamraju, R., Taylor, J., and Zimmerman, P.: A global-model of natural volatile organic-compound emissions, *J. Geophys. Res.-Atmos.*, 100, 8873–8892, 1995.
- Guenther, A., Karl, T., Harley, P., Wiedinmyer, C., Palmer, P. I., and Geron, C.: Estimates of global terrestrial isoprene emissions using MEGAN (Model of Emissions of Gases and Aerosols from Nature), *Atmos. Chem. Phys.*, 6, 3181–3210, <https://doi.org/10.5194/acp-6-3181-2006>, 2006.
- Guenther, A.: Biological and chemical diversity of biogenic volatile organic emissions into the atmosphere, *ISRN Atmospheric Sciences*, 27 pp., <https://doi.org/10.1155/2013/786290>, 2013.
- Guenther, A. B., Monson, R. K., and Fall, R.: Isoprene and monoterpene emission rate variability – Observations with Eucalyptus and emission rate algorithm development, *J. Geophys. Res.-Atmos.*, 96, 10799–10808, 1991.
- Guenther, A. B., Zimmerman, P. R., Harley, P. C., Monson, R. K., and Fall, R.: Isoprene and Monoterpene Emission Rate Variability – Model Evaluations and Sensitivity Analyses, *J. Geophys. Res.-Atmos.*, 98, 12609–12617, 1993.
- Guenther, A. B., Jiang, X., Heald, C. L., Sakulyanontvittaya, T., Duhl, T., Emmons, L. K., and Wang, X.: The Model of Emissions of Gases and Aerosols from Nature version 2.1 (MEGAN2.1): an extended and updated framework for modeling biogenic emissions, *Geosci. Model Dev.*, 5, 1471–1492, <https://doi.org/10.5194/gmd-5-1471-2012>, 2012.
- Guimberteau, M., Ronchail, J., Espinoza, J. C., Lengaigne, M., Sultan, B., Polcher, J., Drapeau, G., Guyot, J. L., Ducharne, A., and Ciais, P.: Future changes in precipitation and impacts on extreme streamflow over Amazonian sub-basins, *Environ. Res. Lett.*, 8, 014040, <https://doi.org/10.1088/1748-9326/8/1/014035>, 2013.
- IPCC Climate Change 2013: The Physical Science Basis, Contribution of Working Group I to the Fifth Assessment Report of the Intergovernmental Panel on Climate Change, edited by: Stocker, T. F., Qin, D., Plattner, G. K., Tignor, M., Allen, S. K., Boschung, J., Nauels, A., Xia, Y., Bex, V., and Midgley, P. M., Cambridge University Press, Cambridge, UK and New York, NY, USA, 1535 pp., 2013.
- Keenan, T., Niinemets, Ü., Sabate, S., Gracia, C., and Peñuelas, J.: Process based inventory of isoprenoid emissions from European forests: model comparisons, current knowledge and uncertainties, *Atmos. Chem. Phys.*, 9, 4053–4076, <https://doi.org/10.5194/acp-9-4053-2009>, 2009.
- Krinner, G., Viovy, N., de Noblet-Ducoudre, N., Ogee, J., Polcher, J., Friedlingstein, P., Ciais, P., Sitch, S., and Prentice, I.: A dynamic global vegetation model for studies of the coupled atmosphere-biosphere system, *Global Biogeochem. Cy*, 19, GB1015, <https://doi.org/10.1038/srep04364>, 2005.
- Lavoir, A.-V., Staudt, M., Schnitzler, J. P., Landais, D., Massol, F., Rocheteau, A., Rodriguez, R., Zimmer, I., and Rambal, S.: Drought reduced monoterpene emissions from the evergreen Mediterranean oak *Quercus ilex*: results from a through-fall displacement experiment, *Biogeosciences*, 6, 1167–1180, <https://doi.org/10.5194/bg-6-1167-2009>, 2009.
- Lichtenthaler, H. K., Schwender, J., Disch, A., and Rohmer, M.: Biosynthesis of isoprenoids in higher plant chloroplasts proceeds via a mevalonate-independent pathway, *FEBS Lett.*, 400, 271–274, 1997.
- Llusià, J., Peñuelas, J., Alessio, G., and Estiarte, M.: Contrasting species specific, compound specific, seasonal and interannual responses of foliar isoprenoid emissions to experimental drought in a Mediterranean shrubland, *Int. J. Plant Sci.*, 169, 637–645, 2008.
- Loreto, F. and Fineschi, S.: Reconciling functions and evolution of isoprene emission in higher plants, *New Phytol.*, 206, 578–582, 2015.
- Loreto, F. and Schnitzler, J.-P.: Abiotic stresses and induced BVOCs, *Trends Plant Sci.*, 15, 154–166, 2010.
- Müller, J.-F., Stavrou, T., Wallens, S., De Smedt, I., Van Roozendael, M., Potosnak, M. J., Rinne, J., Munger, B., Goldstein, A., and Guenther, A. B.: Global isoprene emissions estimated using MEGAN, ECMWF analyses and a detailed canopy environment model, *Atmos. Chem. Phys.*, 8, 1329–1341, <https://doi.org/10.5194/acp-8-1329-2008>, 2008.
- Pacifico, F., Harrison, S. P., Jones, C. D., and Sitch, S.: Isoprene emissions and climate, *Atmos. Environ.*, 43, 6121–6135, 2009.
- Pegoraro, E., Rey, A., Malhi, Y., Bobich, E., Barron-Gafford, G., Grieve, A., and Murthy, R.: Effect of CO<sub>2</sub> concentration and vapour pressure deficit on isoprene emission from leaves of *Populus deltoides* during drought, *Funct. Plant Biol.*, 31, 1137–1147, 2004.
- Peñuelas, J. and Staudt, M.: BVOCs and global change, *Trends Plant Sci.*, 15, 133–144, 2010.
- Peñuelas, J., Llusià, J., Asensio, D., and Munné-Bosch, S.: Linking isoprene with plant thermotolerance, antioxidants, and monoterpene emissions, *Plant Cell Environ.*, 28, 278–286, 2005.
- Petron, G., Harley, P. C., Greenberg, J., and Guenther, A. B.: Seasonal temperature variations influence isoprene emission, *Geophys. Res. Lett.*, 28, 1707–1710, 2001.
- Polade, S. D., Pierce, D. W., Cayan, D. R., Gershunov, A., and Dettinger, M. D.: The key role of dry days in changing regional climate and precipitation regimes, *Sci. Rep.*, 4, 4364, <https://doi.org/10.1038/srep04364>, 2014.
- Potosnak, M. J., LeStourgeon, L., Pallardy, S. G., Hosman, K. P., Gu, L., Karl, T., Geron, C., and Guenther, A. B.: Observed and modeled ecosystem isoprene fluxes from an oak-dominated temperate forest and the influence of drought stress, *Atmos. Environ.*, 84, 314–322, 2014.
- Rodriguez-Calcerrada, J., Buatois, B., Chiche, E., Shahin, O., and Staudt, M.: Leaf isoprene emission declines in *Quercus*

- pubescens seedlings experiencing drought – Any implication of soluble sugars and mitochondrial respiration?, *Environ. Exp. Bot.*, 85, 36–42, 2013.
- Santonja, M., Fernandez, C., Gauquelin, T., and Baldy, V.: Climate change effects on litter decomposition: intensive drought leads to a strong decrease of litter mixture interactions, *Plant Soil*, 393, 69–82, 2015.
- Saunier, A., Ormeño, E., Boissard, C., Wortham, H., Temime-Roussel, B., Lecareux, C., Armengaud, A., and Fernandez, C.: Effect of mid-term drought on *Quercus pubescens* BVOCs' emission seasonality and their dependency on light and/or temperature, *Atmos. Chem. Phys.*, 17, 7555–7566, <https://doi.org/10.5194/acp-17-7555-2017>, 2017.
- Sharkey, T. D. and Loreto, F.: Water-stress, temperature, and light effects on the capacity for isoprene emission and photosynthesis of kudzu leaves, *Oecologia*, 95, 328–333, 1993.
- Simon, V., Dumergues, L., Solognac, G., and Torres, L.: Biogenic emissions from *Pinus halepensis*: a typical species of the Mediterranean area, *Atmos. Environ.*, 74, 37–48, 2005.
- Tani, A., Tozaki, D., Okumura, M., Nozoe, S., and Hirano, T.: Effect of drought stress on isoprene emission from two major *Quercus* species native to East Asia, *Atmos. Environ.*, 45, 6261–6266, 2011.
- Tognetti, R., Longobucco, A., Miglietta, F., and Raschi, A.: Transpiration and stomatal behaviour of *Quercus ilex* plants during the summer in a Mediterranean carbon dioxide spring, *Plant Cell Environ.*, 21, 613–622, 1998.
- Velikova, V., Sharkey, T. D., and Loreto, F.: Stabilization of thylakoid membranes in isoprene-emitting plants reduces formation of reactive oxygen species, *Plant Signal. Behav.*, 7, 139–141, 2012.
- Von Caemmerer, S. and Farquhar, G. D.: Some relationships between the biochemistry of photosynthesis and the gas-exchange of leaves, *Planta*, 153, 376–387, 1981.
- von Kuhlmann, R., Lawrence, M. G., Pöschl, U., and Crutzen, P. J.: Sensitivities in global scale modeling of isoprene, *Atmos. Chem. Phys.*, 4, 1–17, <https://doi.org/10.5194/acp-4-1-2004>, 2004.
- Warszawski, L., Frieler, K., Huber, V., Piontek, F., Serdeczny, O., and Schewe, J.: The Inter-Sectoral Impact Model Intercomparison Project (ISI-MIP): Project framework, *P. Natl. Acad. Sci. USA*, 111, 3228–3232, 2014.
- Wiberley, A., Linskey, A., Falbel, T., and Sharkey, T.: Development of the capacity for isoprene emission in kudzu, *Plant. Cell Environ.*, 28, 898–905, 2005.
- Zheng, Y., Unger, N., Barkley, M. P., and Yue, X.: Relationships between photosynthesis and formaldehyde as a probe of isoprene emission, *Atmos. Chem. Phys.*, 15, 8559–8576, <https://doi.org/10.5194/acp-15-8559-2015>, 2015.
- Zobler, L.: A world soil file for global climate modelling, NASA Technical Memorandum, NASA 87802, New York, USA, 1986.